Master Thesis

in the department of

Materials Science and Engineering

to obtain the degree of Master of Science

at the

Delft University of Technology

Physicochemical characterization of corrosion inhibition on galvanized steel surfaces

Organic coatings and green corrosion inhibitors

by

M.V.E. Ankora (4630440)

Thesis Committee:

Dr. ir. J. M. C. Mol, TU Delft (Chairman)
Laura-Lynn Fockaert, TU Delft
Mats Meeusen, TU Delft
Dr. ir. Marcel Hermans, TU Delft

Abstract

Conversion coatings are generally required to enhance organic coating adhesion and corrosion resistance on galvanized steel[1]. Until a few decades ago, chromate conversion coatings were the most common conversion coatings in the industry owing to their exceptional performance in this regard. However, the adverse effects associated with hexavalent chromium as found in chromate conversion coatings and certain corrosion inhibitor pigments are now widely known. As a result, various initiatives have been deployed around the globe to restrict and regulate the use of hexavalent chromium. Finding suitable alternatives for chromate conversion coatings has therefore become one of the most pertinent research topics of the moment in the field of corrosion protection.

A number of chromium-free conversion coatings have been found to show comparable corrosion resistance relative to chromate conversion coatings. For galvanized steel, conversion coatings based on zirconium and titanium have been found to be suitable alternatives to chromium [1, 2]. Organic additives may be incorporated in these conversion treatment solutions for galvanized steel to enhance the adhesion of organic coatings to the substrate. The effect of a given organic additive is highly dependent on the surface composition of the substrate as has been observed with the polymers polyacrylic acid (PAA), polyvinyl alcohol (PVA) and polyvinyl pyrrolidone (PVP) on hot-dip galvanized steel and a Zn-Mg-Al alloy coated steel studied in this project.

The durability of corrosion protection may also be enhanced by embedding corrosion inhibitors in the organic coating. An increased concern for sustainability and environmental-friendliness, has resulted in a global effort toward developing and using corrosion inhibitors which are safe for the environment and for human health. The electrochemical behaviour of galvanized steel in electrolytes with green inhibitors based on silicates, phosphates, zinc oxide and calcium at various concentrations are investigated.

This project considers a multi-layer corrosion protection coating system comprising a conversion layer based on Zr/Ti cations and adhesion-enhancing polymer additives, and an organic coating embedded with 'green' corrosion inhibitors. The overarching aim is to investigate and establish new knowledge regarding the effect of polymer additives in conversion coatings on the adhesion of organic coatings as well as the identification of suitable green corrosion inhibitors. The outcome is an indication of which types of polymer additives and corrosion inhibitors work best for the two substrates tested - MagiZinc® and hot-dip galvanized steel, both supplied by Tata Steel BV.

Contents

List of Figures

Chapter 1

Introduction

1.1 Current state of the art

Steel is among the most produced man-made materials in the world. Thousands of tons of this material are produced globally every year. In 2017, the global Apparent Steel Use (ASU), which defines the production plus net imports of finished steel products [3] amounted to 1,587 million tonnes [4]. It comprises an integral part of infrastructure, building materials, as well as consumer product packaging among others. This is due to its high tensile strength and low cost. However, every year, a lot is spent to repair or replace steel due to damage from corrosion. For this reason, finding ways to protect steel from corrosion is of prime importance for the various applications of steel.

According to the IMPACT study published in 2016 by the National Association of Corrosion Engineers, corrosion was reported to have cost the global economy US $ 2.5 trillion which amounted to 3.3% of the global world product that year [5]. It is also proposed in this report that should all of the corrosion control tools that are available be implemented globally, savings of up to 15 to 35% of corrosion costs could be realized.

Although galvanized steel has improved corrosion protection compared to bare steel, zinc is susceptible to environmental degradation resulting in the formation of 'white rust' which eventually leads to the depletion of the protective zinc layer. For this reason, further protection of galvanized steel is required and this is usually provided through a multi-layer coating system. This typically comprises surface pretreatment and then application of organic coating layers which usually comprise a primer layer and a topcoat. A lot of research effort has been directed towards maximizing the durability of the adhesion of the organic layer to the substrate. Recent studies have explored the use of polymer additives to improve corrosion protection at the interface [1]. Though these additives are usually incorporated at low concentrations, it is likely that their presence at the interface influences coating adhesion strength. Despite this, there exists very limited research into the effect of organic additives in the conversion treatment solution on the adhesion of organic coatings to the treated surface. This thesis is intended to fill a part of that knowledge gap.

While working toward the aim of high-performing corrosion protection, it is important to consider the effect of the technologies being investigated and developed on the environment. It is for this reason that chromate-free pretreatments will be the focus of this thesis, in line with the global effort towards minimizing the use of hexavalent chromium. The use of chromium, a substance which due to its high performance serves as a benchmark for corrosion protection, has been subject to ever stricter regulation due to the hazard it poses to health and the environment. For protection of industrial galvanized steel, zirconium- and titanium-based treatments have been found to be viable alternatives [1]. These treatments decrease the total material processing time and also allow for thinner coatings to be used[2].

Even further corrosion protection may be achieved by embedding corrosion inhibitors in the organic coating. These inhibiting particles interact with the corrosion system to reduce the current density of either the cathodic or anodic reaction or both. Also in the field of corrosion inhibitors, research is geared

towards inhibitors which have minimal adverse effects on health and the environment. Inhibitors that fulfill these requirements are termed 'green inhibitors'. In this project, green corrosion inhibitors based on silicate, polyphosphate, and calcium oxide compounds are investigated. An in-depth look will be given to the electrochemical behaviour of these green inhibitors in saltwater. And it is intended that the results obtained through this investigation reveal more knowledge about the corrosion protection mechanism of this class of inhibitors.

1.2 Scientific motivation and research approach

Organic coatings are applied to galvanized steel surfaces to enhance corrosion resistance and thus extend the lifetime of the substrate. A consequent requirement is that the applied coatings remain on the steel surface especially in corrosive environments for the duration of the intended lifetime.

While commercial conversion coatings make wide use of hexafluorozirconic acid (H_2ZrF_6), hexafluorotitanic acid (H_2TiF_6) and inorganic and/or organic additives, the specific contributions of the various cations and polymer additives are not yet clearly understood. It has been shown that the final performance of conversion coatings is highly substrate dependent due to differences in thickness and elemental distribution that are possible with each type of metal substrate [6]. In view of this, the objective of this thesis is to gain insight into the types of organic additives which improve adhesion between a galvanized steel substrate and an organic coating and how modifications to these variables affect electrochemical behaviour and corrosion resistance specifically. The research questions that we aim to address in this thesis are:

1. How do titanium and zirconium compare as conversion coatings with regard to improving adhesion of organic coatings to the metal surface?
2. How is adhesion on a galvanized steel surface influenced by incorporating organic additives in the conversion layer?
3. In what way, if at all, is corrosion behaviour affected by the corrosion inhibitors studied?
4. Which green corrosion inhibitors of those studied are most suitable for corrosion protection protection on MagiZinc?

The research approach will be a consideration of a multi-layer coating system as described in the diagram below:

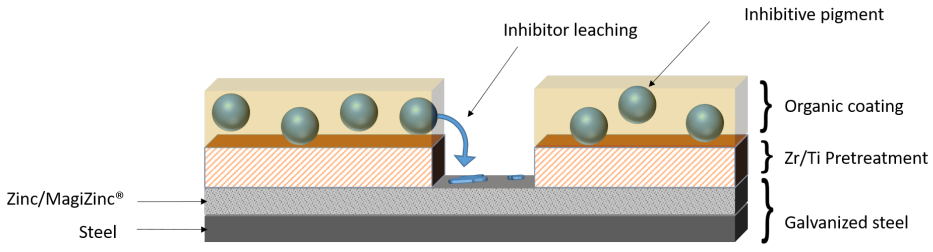

Figure 1.1: The system investigated in this project comprises galvanized steel coated with an organic paint in which green corrosion inhibitive pigments have been incorporated

To isolate the effects of each variable, however, this study will be carried out in two parts. The first part (Figure 1.2) examines the effect of polymer additives on the physical and chemical properties of the substrate and how that in turn affects coating adhesion. This part of the study involves, in the fist step, an evaluation of the changes to the surface chemistry and morphology as a function of the conversion solution with which the samples are treated. After pretreatment, samples will then be coated with a thin model polyester coating to which no inhibitors have been added. The pull-off adhesion strength of these coated samples will then be measured and compared against the results obtained from the aforementioned surface analysis.

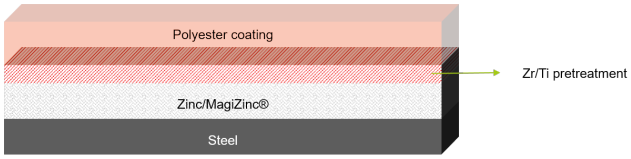

Figure 1.2: Effect of polymer additives on adhesion

The second part (Figure 1.3)will be an investigation into inorganic green corrosion inhibitors for galvanized steel surfaces. Samples will be tested in various concentrations of each of the inhibitors selected for this study. From these tests, the inhibitor efficiency and the manner of corrosion inhibition provided by each of these inhibitors will be evaluated.

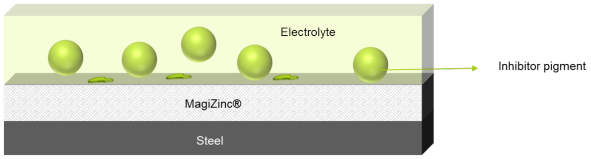

Figure 1.3: Effect of inorganic green corrosion inhibitors on electrochemical behaviour

Chapter 2

Fundamentals of corrosion

2.1 Fundamentals of corrosion

Corrosion is a process which converts metal atoms to ionic species of a higher oxidative state. For corrosion to occur, four main things are required:

1. Anode
2. Cathode
3. Electrolyte
4. Electron path

Together, the above four factors comprise an electrochemical cell, and more specifically in the case of corrosion, a *corrosion cell*.

Anode: At the anode, the corroding metal is oxidized to its ionic state. This, in the case of steel, involves the oxidation of zinc and iron respectively as follows:

$$\mathrm{Zn} \longrightarrow \mathrm{Zn^{2+}} + 2\,\mathrm{e^-} \tag{2.1}$$

$$\mathrm{Fe} \longrightarrow \mathrm{Fe^{2+}} + 2\,\mathrm{e^-} \tag{2.2}$$

The standard reduction potential of the oxidation reaction for zinc, at $-0.76\,\mathrm{V}$, is much lower than that of iron at $-0.41\,\mathrm{V}$ which makes it an ideal sacrificial anode for the corrosion protection of iron. Following the above reactions, further hydrolysis and oxidation reactions occur such as:

$$\mathrm{Fe^2} + \mathrm{H_2O} \longrightarrow \mathrm{FeOH^+} + \mathrm{H^+}$$

$$\mathrm{Fe^{2+}} \longrightarrow \mathrm{Fe^{3+}} + \mathrm{e^-}$$

which lead to the formation of metal hydroxides and oxides. With galvanized steel, what happens is that at the initial pristine state, zinc serves as barrier protection for iron. Subsequently, with sufficient oxygen and moisture, zinc oxidizes according to equation (2.1). This leads to the formation of ZnO and $\mathrm{ZnCl_2 \cdot 4\,Zn(OH)_2}$ also known as *white rust*, a porous, non-adherent, powdery white substance which is thought to enable further corrosion [7]. Once the zinc layer is depleted, iron oxidation proceeds as in equation (2.2). From this reaction, $\mathrm{OH^-}$ are formed and for this reason, acidic conditions accelerate the rate of rusting of iron.

Cathode: The electrons released in the anodic reaction are consumed at the cathode. Cathodic reactions vary depending on the ambient conditions. Possible reactions include:

$$O_2 + 2\,H_2O + 4\,e^- \longrightarrow 4\,OH^-$$

$$O_2 + 4\,H^+ + 4\,e^- \longrightarrow 2\,H_2O$$

$$2\,H^+ + 2\,e^- \longrightarrow H_2$$

Electrolyte: Positive charges flow through the electrolyte from the anode to the cathode in the form of the cations produced in the anodic reaction.

Electron path: Electrons are transported via metallic conduction from the anodic site to the cathodic site.

The corrosion cell for iron in an oxygenated, moist environment is shown in Fig. 2.1. Iron serves as the electron path between anodic and cathodic sites on its surface. Ions migrate between electrodes through the electrolyte which in this case is water. The oxides formed by the oxidation of iron by oxygen lead to the formation of iron oxides which are deposited next to the anodic site as red non-adherent substance also called *red rust*.

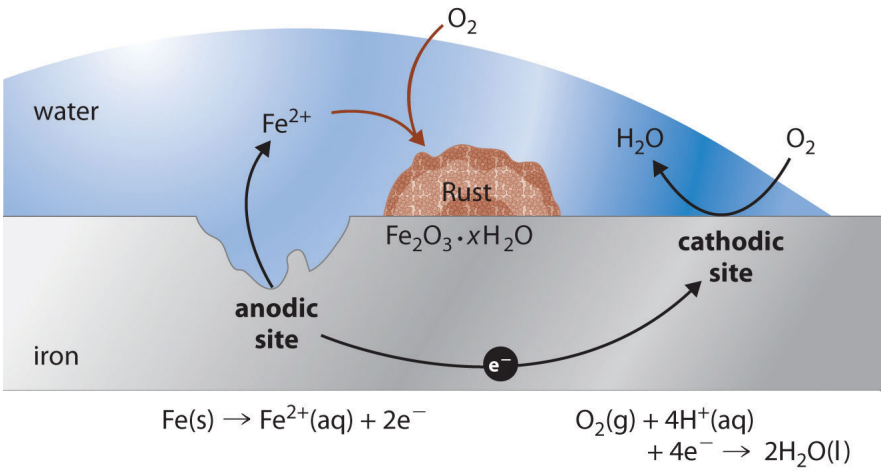

Figure 2.1: Corrosion of Iron

Once these components are in place, corrosion reactions commence which generate electrical energy. This is quantified as follows:

$$\begin{aligned} \text{Electrical energy} &= \text{volts} \times \text{current} \times \text{time} \\ &= \text{volts} \times \text{coulombs} \\ &= V \times Q \end{aligned} \tag{2.3}$$

where

$$Q = n \times F \tag{2.4}$$

where
n is the number of moles of electrons involved in the reaction
F is Faraday's constant which represents the amount of electric charge per mole of electrons = 96485.33

C mol^{-1}
V, the electromotive force of the cell is the amount of energy generated per unit.

2.2 Anodic dissolution

The half of the corrosion reaction in which the surface atoms of the metal are oxidized and then freed from the bulk metal into the electrolyte is termed as *anodic dissolution*. Three mechanisms are said to be involved in anodic dissolution [8]:

1. Acid-catalyzed anion-ligand mechanism:
   $M + A^- \longrightarrow MOH_{ads} + H^+ + e^-$
   $MOH_{ads} \longrightarrow {MOH_{aq}}^+ + e^-$
2. Base-catalyzed aquo-ligand mechanism:
   $M \longrightarrow {M_{ads}}^+ + e^-$
   ${M_{ads}}^+ \longrightarrow {M_2}^+{}_{aq} + e^-$
3. Water-catalyzed hydroxo-ligand mechanism:
   $M + H_2O \longrightarrow MOH_{ads} + H^+ + e^-$
   $MOH_{ads} \longrightarrow {MOH_{aq}}^+ + e^-$

Anodic dissolution ultimately results in significant loss of material. This eventually renders the metal no longer fit for the purpose for which it was intended. A corroding metal in solution reaches an equilibrium potential at which the rate of the anodic reaction equals that of the cathodic reaction. This is called the **corrosion potential** or the **open-circuit potential**. The current generated by the dissolution reaction at the open-circuit potential is called the **corrosion current**.

Displacing the potential in the positive direction increases the rate of the anodic reaction. Positive displacement of the potential is called **anodic polarization**. Negative displacement of the potential drives the rate of the cathodic reaction higher and is called **cathodic polarization**.

2.3 Pourbaix diagrams and polarization curves

To fully grasp the thermodynamics and kinetics of corrosion and to formulate techniques for its characterization and application to corrosion protection of metals, we take a look at Pourbaix diagrams and polarization curves. Polarization curves, an example of which is shown in Figure 2.2, graph the potential and passivation behaviour of a specific metal as a function of corrosion density (the amount of current per unit area of cross-section). The corrosion density is directly proportional to the rate of the corrosion reaction; the higher the rate of corrosion, the higher the observed current density. This proportionality is defined by the Tafel equation:

$$i = nFkCe^{\pm\alpha F\frac{\eta}{RT}} \tag{2.5}$$

where
k is the rate constant for the electrode reaction,
C is the concentration of the reactive species at the electrode,
α is the charge transfer coefficient,

R is the universal gas constant and,
T is the absolute temperature.

As shown in Figure 2.2 below, the corrosion current, i_{corr}, and corrosion potential, E_{corr}, are determined by extrapolating the Tafel lines for the cathodic and anodic branches of the corrosion reaction. The coordinates of the point of intersection of the lines correspond to the potential at which the anodic reaction rate is equal to the cathodic reaction rate and therefore, there is no net current flow to or from the metal. From these curves, information regarding the conditions under which corrosion occurs as well as those that enable passivation, the transpassive region, and other regimes may be obtained.

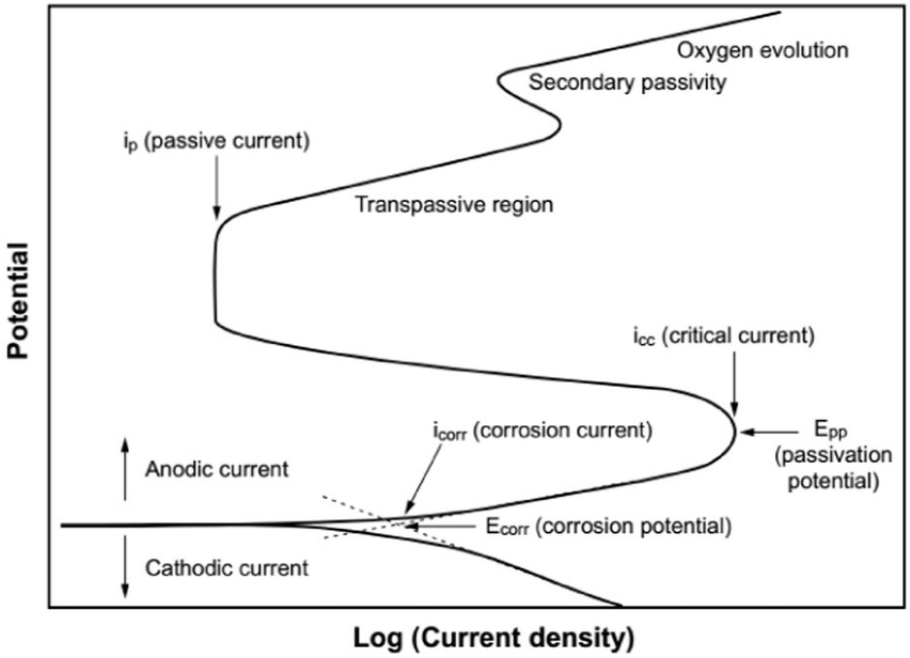

Figure 2.2: Polarization diagram of an active-passive metal

Pourbaix diagrams, on the other hand, relate the electrochemically stable states of an element in an aqueous system as a function of potential versus pH. A line demarcating the boundary between two regions indicates conditions at which both species represented on either side of the line exist in equilibrium. A similar state of equilibrium is represented by the vertex of three or more lines. The Pourbaix diagrams for iron and zinc are shown below in Figures 2.3a and 2.3b. The region in which the metal is represented in its elemental form corresponds to the range of conditions where the potential is below the oxidation potential i.e. cathodic potential and thus, is said to be cathodically protected.

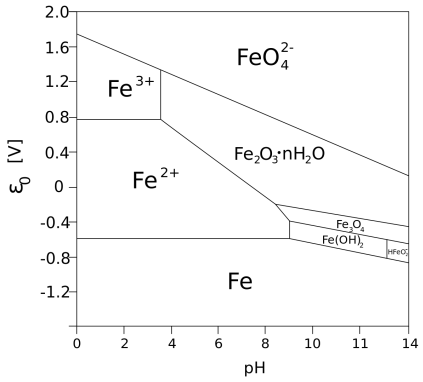

(a) Potential-pH equilibrium (Pourbaix) diagram for iron-water [9]

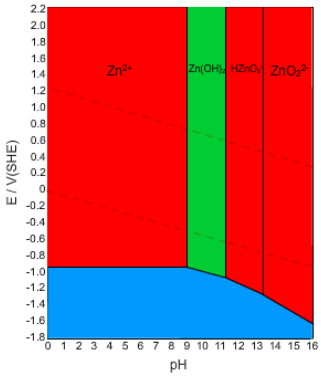

(b) Potential-pH equilibrium (Pourbaix) diagram for zinc

Cathodic protection is most commonly provided by connecting the metal to be protected to a less electrochemically noble metal. As a reference, Figure 2.4 shows the standard reduction potentials of some common metals relative to hydrogen. The more noble the metal, the more positive is its reduction potential. In a cathodic protection set-up, the more active material sacrificially protects the metal of interest by acting as an anode in the electrochemical cell formed by connecting the two metals. Various types of cathodic protection are available; these include galvanization, impressed current systems or hybrids of the two systems. This thesis deals only with steels galvanized via a direct coating of zinc or a zinc alloy.

oxidised form A_{Ox}	$+ n e^-$	reduced form A_{Red}	E° / V
$Li^+_{(aq)} + e^-$	⇌	$Li_{(s)}$	-3.04
$K^+_{(aq)} + e^-$	⇌	$K_{(s)}$	-2.92
$Na^+_{(aq)} + e^-$	⇌	$Na_{(s)}$	-2.71
$Zn^{2+}_{(aq)} + 2\,e^-$	⇌	$Zn_{(s)}$	-0.76
$Pb^{2+}_{(aq)} + 2\,e^-$	⇌	$Pb_{(s)}$	-0.13
$2\,H^+_{(aq)} + 2\,e^-$	⇌	$H_{2(g)}$	0.00
$N_{2(g)} + 8\,H^+_{(aq)} + 6\,e^-$	⇌	$2\,NH^+_{4(aq)}$	+0.27
$Cu^{2+}_{(aq)} + 2\,e^-$	⇌	$Cu_{(s)}$	+0.34
$I_{2(s)} + 2\,e^-$	⇌	$2\,I^-_{(aq)}$	+0.54
$O_{2(aq)} + 2\,H^+_{(aq)} + 2\,e^-$	⇌	$H_2O_{2(aq)}$	+0.68
$Fe^{3+}_{(aq)} + e^-$	⇌	$Fe^{2+}_{(aq)}$	+0.77
$NO^-_{3(aq)} + 4\,H^+_{(aq)} + 3\,e^-$	⇌	$NO_{(g)} + 2\,H_2O_{(l)}$	+0.96
$O_{2(g)} + 4\,H^+_{(aq)} + 4\,e^-$	⇌	$2\,H_2O_{(l)}$	+1.23
$Cl_{2(g)} + 2\,e^-$	⇌	$2\,Cl^-_{(aq)}$	+1.36
$Cr_2O^{2-}_{7(aq)} + 14\,H^+_{(aq)} + 6\,e^-$	⇌	$2\,Cr^{3+}_{(aq)} + 7\,H_2O_{(l)}$	+1.36
$MnO^-_{4(aq)} + 8\,H^+_{(aq)} + 5\,e^-$	⇌	$Mn^{2+}_{(aq)}$	+1.49
$H_2O_{2(aq)} + 2\,H^+_{(aq)} + 2\,e^-$	⇌	$2\,H_2O_{(l)}$	+1.78
$F_{2(g)} + 2\,e^-$	⇌	$2\,F^-_{(aq)}$	+2.87

Figure 2.4: Standard reduction potentials relative to hydrogen

2.4 Corrosion protection of galvanized steel

2.4.1 Passivity

Passivity is observed in all metals and alloys and is a phenomenon on which many corrosion protection techniques are based. As a result of reactions with oxygen and water, metal oxidation occurs which leaves a thin film of oxide products on the metal surface. In some instances, the oxide formed is highly stable and adheres strongly to the parent metal. It is able to resist further oxidation and thus, protects the underlying metal from corrosion. Such a layer is called a passive layer and the metal is said to be in a state of **passivity**.

This is not always the case. Contrary to the passivating oxide layers formed by many other transition metals, the oxide layers formed by iron are friable and tend to flake off the surface due to the larger volume of the oxide relative to the parent metal. This exposes the iron underneath allowing corrosion to proceed deeper into the metal until, given enough time under these conditions, the entire specimen is corroded. It is for this reason that the protection of steel against corrosion is necessary.

In the passivated state, the rate of the oxidation reaction is significantly slowed and current flow also significantly reduced. This phenomenon is very clearly shown in polarization curves, where in the region of passivity, the graph is vertical as shown in Figure 2.2. The passive current density (i_p) is also orders of magnitude lower than i_{corr}.

According to Revie and Uhlig [10], there are two types of passivity:

> Type 1 - "A metal is passive if it substantially resists corrosion in a given environment resulting from marked anodic polarization". This is valid for low corrosion rates at noble potentials.
>
> Type 2 - "A metal is passive if it substantially resists corrosion in a given environment despite a marked thermodynamic tendency to react." This is valid for low corrosion rates even at active potentials.

For corrosion protection, passivation may be induced by incorporating oxidizing species such as chromates, aluminates and nitrates. These species reinforce the passivation behaviour of the metal surface by their ability to spontaneously form stable, adherent oxides upon oxidation.

2.4.2 Galvanization

Zinc is the most widely used galvanizing material for steel. This is because in addition to providing cathodic protection, zinc also forms corrosion products which are able to provide protection even at defects that go down to the metal surface and at sharp edges [11, 12]. A zinc coating may be deposited on a steel substrate in a variety of ways. These include:

- Hot-dip galvanizing (GI)
  As the name suggests, the conventional hot-dip galvanizing process involves immersing steel in a molten zinc bath at a temperature of around 450 to 490 ℃[13] where the zinc reacts and bonds with the steel surface. The primary advantage of this means of galvanization is that a uniform minimum thickness of zinc is guaranteed. Hot-dip galvanizing may be performed in two different ways: batch

or continuous hot-dip galvanizing. Batch hot-dip galvanization is especially advantageous when the specimens to be galvanized are pre-formed and complex-shaped objects. The batch process allows the molten zinc to cover all possible surfaces. For wires, pipe and sheets a continuous galvanization process is applicable in which there is a constant feed of material be coated into the bath. This type of hot-dip galvanizing has the advantage of being more tunable. The velocity of the wire, pipe or sheet through the bath may be adjusted to allow accurate control of coating thickness among other properties of the zinc coating.

- Zinc electroplating
  In this process, zinc is electrodeposited on the surface by immersion of the steel in a solution of zinc ions and other additives for deposition enhancement. An electric current is then applied which induces deposition of zinc from the electrolyte on the steel surface.

- Thermal spray/ Metallizing
  In this process, semi-molten zinc is sprayed onto the metal surface and then allowed to solidify to form a protective coating.

- Sherardizing and Thermal diffusion
  Sherardizing involves heating up the steel in a closed rotating receptacle containing zinc. At temperatures above 300 ℃, the zinc powder vaporizes and then diffuses to the steel surface where it reacts to form a diffusion-bonded Fe-Zn surface layer.

- Mechanical plating
  Mechanical plating is performed at room temperature. Similar to sherardizing and thermal diffusion, the coating process is carried out in a rotating drum but in this case, with the addition of glass beads as impact transfer media. The drum is then rotated i,parting mechanical energy to the glass beads which in turn cold weld the zinc to the substrate.

The two galvanized steels studied in this thesis, are hot-dip galvanized steels supplied by Tata Steel. The first kind is a steel sheet with the conventional zinc coating (commonly referred to by the abbreviation GI) while the other coating is a zinc-magnesium-aluminum alloy sold under the Tata Steel trade name as MagiZinc® (abbreviated from this point further as MZ).

The surface composition of GI comprises zinc (Zn) with 0.20 wt% aluminum (Al) and about 0.01 wt% of iron (Fe) due to some dissolution of Fe in the bath during the galvanization process. When galvanization is performed in a pure zinc bath, brittle Fe-Zn intermetallic phases rapidly form on the surface leading to poor adhesion of the zinc coating. Al prevents this in two ways: first, it acts as an inhibitor to the Fe-Zn phase formation process. Secondly, at the correct addition levels, Al causes the rapid formation of a uniform Al-Zn-Fe layer with 45% Al, 35% Fe and 20% Zn. This serves as a base for strong adhesion of the zinc coating to the substrate [14].

Although conventional galvanization efficiently fulfills the role of corrosion protection for steel, a lot of work has been done towards achieving thinner coatings with comparable or even better performance than the traditional zinc coated steel. This is in order to optimize process costs as well as to reduce energy consumption and carbon emissions. Of the various alloying elements studied, magnesium appears to provide the best results. It has been established that the inclusion of Mg, like Al, prevents the formation of a Zn-Fe alloy layer and of Zn oxide during galvanizing [15]. The addition of Mg also speeds up coating formation and significantly improves the corrosion resistance of the coating .

Ideally, coating steel with a zinc-magnesium alloy requires a physical vapour deposition procedure [11]. To create such a coating via the hot-dipping process, theh addition of Al is then required to prevent the formation of dross which has a detrimental effect on the service lifetime of bath hardware as well as on

coating quality in terms of defect formation [16]. Additionally, aluminum provides further protection capability due to its passivation ability.

Chapter 3

Corrosion protection of galvanized steel: Chromium-free pretreatments

3.1 The need for pretreatments

Organic coatings are commonly used as a final protection layer against corrosion of galvanized steel. However, these coatings are liable to failure by **cathodic delamination**. This occurs when electrolytes permeate to the coating-substrate interface and initiate anodic dissolution:

$$\mathrm{Fe} \longrightarrow \mathrm{Fe}^{2+} + 2\,\mathrm{e}^- \tag{3.1}$$

The electrons lost by the metal migrate to cathodic sites and there facilitate the reduction of oxygen which produces hydroxide ions, peroxide ions and related species:

$$\mathrm{O_2} + 4\,\mathrm{e}^- + 2\,\mathrm{H_2O} \longrightarrow 4\,\mathrm{OH}^-$$

$$\mathrm{O_2} + \mathrm{H_2O} + 2\,\mathrm{e}^- \longrightarrow \mathrm{HO_2}^- + \mathrm{OH}^-$$

$$2\,\mathrm{HO_2} \longrightarrow 2\,\mathrm{OH}^- + \mathrm{O_2}$$

$$\mathrm{O_2} + \mathrm{e}^- \longrightarrow {}^*\mathrm{O_2}^-$$

Build-up of hydroxide and peroxide ions which are intermediate products of the reduction reaction leads to a local pH increase at these sites. The aggressive intermediate species created during the oxygen reduction process, especially peroxide and its decomposition products, chemically attack the coating and in this way weaken adhesion between the coating and substrate [17–20]. As a result, cathodic delamination occurs [21].

One way of reducing the rate of cathodic delamination is by the application of conversion coatings. These work in a variety of ways. They can provide a lower overpotential for the oxygen reduction reaction and in this way reduce the rate of alkalinization of the surface. They may also be capable of forming interfacial bonds with organic coatings that are much less susceptible to chemical attack by products from the oxidation reaction. Mechanics-wise, many conversion coatings increase the roughness of the surface thereby providing more surface area for the formation of interfacial bonds.

Surface pre-treatments modify the surface and include such treatments as grinding, etching and conversion coatings which prepare the surface for subsequent coating and/or deposit some corrosion inhibiting species on the surface. A conversion coating is a layer formed by subjecting a metal to an electrochemical process without the use of an external current which is less susceptible to degradation by aggressive chemical species. It serves to protect the metal from corrosion but also performs the primary role of improving adhesion of subsequently applied paint layers [1]. Subsequent organic layers serve as barrier protection by decreasing the rate of permeation of electrolytes to the metal surface. For organic coatings

to provide said protection, it is necessary that at the interface with the metal surface, minimal contact with electrolytes is allowed. This requires that the applied coating remains adhered especially in corrosive environments. Conversion coatings and organic coatings are therefore widely used to protect galvanized steel from corrosion by increasing the life span of protection from the zinc layer [22].

Conversion treatments on metal are based mainly on metals such as molybdates, chromates and phosphates. Chromate conversion coatings in particular are exceptionally effective at corrosion prevention. They are capable of providing highly effective corrosion protection by virtue of chromium ions in both the 3+ or 6+ oxidation states. Cr^{6+} reduces to Cr^{3+} after a mechanical or chemical breach of the coating, which then reacts with the ambient air to form an insoluble oxide compound, creating a protective coating at the defect site. This mechanism is what provides the self-healing property of chromate conversion coatings. The major disadvantage of chromium is that it poses a hazard to health and the environment. Research has shown that hexavalent chromium causes cancers targeting the kidney, liver, respiratory system, skin and eyes in addition to causing birth defects [23]. For this reason, chromium conversion coatings and other processes involving the use of chromium are now subject to stringent in Europe which has spurred the industry to direct a lot of effort and resources into identifying suitable alternatives.

Phosphating, on the other hand, provides an ideal surface for adhesion but not much by way of corrosion protection. Its high porosity provides a large surface area for the formation of bonds with organic coatings but is also the avenue by which permeation of electrolytes to the metal surface occurs and in this way corrosion performance is compromised. Furthermore, tighter restrictions have been placed on industrial processes involving phosphating due to the toxicity of the effluent to the environment.

3.2 Conversion coating

Two alternatives that have been proven to exhibit performance comparable to chromium and phosphates are zirconium and titanium. Zirconium and titanium are resistant to attack by chlorides and acids and are therefore extensively used in nuclear plants as well as aerospace applications. They are also increasingly found in other metal applications. This is due to the ease with which passive films of TiO_2 and ZrO_2 are formed [24, 25]. These films are instantaneously formed upon exposure of the pure metal to trace amounts of moisture and oxygen and are thus able to prevent further corrosion.

An initial higher relative hydroxide fraction on the metal surface prior to the conversion coating process has been shown by Taheri [26] to have a positive correlation with the deposition of zirconium.

A conversion coating is a layer formed by subjecting a metal to an electrochemical process without the use of an external current. It serves to protect the metal from corrosion but also performs the primary role of improving adhesion of subsequently applied paint layers [1]. A type of conversion coating that was until very recently very widely used is chromate coatings. For steel, chromating is performed on already galvanized steel to protect the zinc layer from white corrosion. However, this type of conversion coating is now subject to heavy regulation due its toxicity. This is because the hexavalent chromium which is employed in the coating process has been found to be a danger to human health especially for those who work with compounds of chromium as is the case in the steel and leather-making industries.

To form a conversion layer, the passive layer that resides on the surface first has to be broken down. This is done by adding ions such as chloride and sulphate to the conversion solution. For zirconium and titanium coatings the ion employed is usually fluoride. The electrolytes used for the conversion processes involving these metals are therefore usually based on H_2TiF_6 and H_2ZrF_6 respectively.

3.3 Chromate-free pretreatments for galvanized steel

For steels with a converted layer, one of the key roles of a subsequent organic coating is to provide additional corrosion protection. Organic coatings prevent/limit corrosion in one or more of the following ways;

- ***Barrier protection.*** It has been proven that paint systems do not protect metal substrates by way of being an impermeable membrane. In fact, many paint systems permit water permeation at a much higher rate than is required for corrosion to take place [27, 28]. Rather, the polymers used in these coatings form films that are able to limit oxygen ingress to the metal surface such that there is an oxygen insufficiency for the cathodic reaction. Some barrier coatings may also serve as an ionic filter by virtue of their high electrolytic resistance.
- ***Cathodic protection.*** When the applied polymer film contains pigments that are anodic compared to the underlying metal substrate, it is able to prevent electronic discharge from the metal to the environment.
- ***Corrosion inhibition.*** Soluble inhibiting moeities can also be incorporated in the paint formulation. In this case, the formulation is designed such that the cured film is able to react with select stimuli (eg. heat, moisture) to establish a passive or inhibitive film on the surface [28]. Many of the inhibitors used for steel are effective only at high concentrations and/or are very toxic and as such are likely to contaminate the surroundings when they leach into the environment. Some of these substances prove to be toxic to environment. Therefore it is necessary to identify less hazardous alternatives.

A key parameter that factors into the ability of a coating to provide these protective properties is its ability to maintain adhesion to the substrate even under prolonged environmental exposure [29]. Although there does not appear to be a consistent correlation between the maintenance of adhesion and the level of corrosion protection provided by a coating, there is, nevertheless, proof that maintaining at least a certain level of adhesion between the coating and the metal substrate limits the spread of corrosion [29]. It has also been observed that corrosion beneath a barrier film can only take place after delamination has occurred [28, 30].

3.4 Fundamentals of intermolecular, surface and interfacial science

Adhesion results from the interplay of a variety of mechanisms. First of all, adhesion requires wetting of the substrate. This describes the ability of a substance such as an organic coating to maintain contact with a solid surface. The degree of wetting is determined by the balance between adhesive and cohesive forces of the liquid. It is quantified by the contact angle which is the angle between the liquid and metal interfaces with air as shown in Figure 3.1. A low contact angle indicates high wetting capability and a high surface energy. Contact angle measurements enable the determination of surface energy due to the correlation of the two parameters as described in the Young-Dupré Equation:

$$\gamma_{SV} = \gamma_{SL} + \gamma_{LV}(\cos\theta) + \pi_e \tag{3.2}$$

where
γ_{SV} is the surface free energy of the solid,

γ_{SL} is the interfacial tension between the solid and the liquid,
θ is the angle of the liquid on the solid surface and
π_e is the equilibrium spreading pressure a measure of the energy released by adsorption if vapor onto the solid surface. The minus sign on this term denotes the consequent loss of surface free energy.

The correlation between wetting and adhesion was studied by deBruyne on various substrates. It was established through these that there was a correlation between the contact angle measured at the liquid-solid interface and adhesion strength. deBruyne observed that as the contact angle between an adhesive in its liquid and a substrate reduces the adhesion strength measured increased. This result confirms the proposed dependence of adhesion strength on wetting.

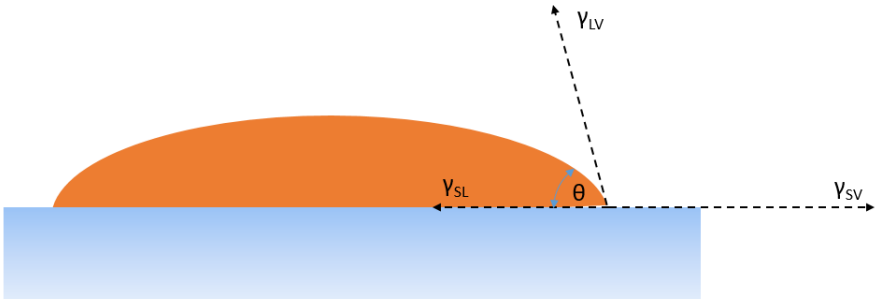

Figure 3.1: Calculation of the Young-Dupré equation

To understand adhesion and the factors that influence it, the fundamental interactions that at surface occur and interfaces must be understood. The methods used to quantify and improve adhesion are based on these principles.

3.4.1 Intermolecular interactions

While there are interactions that are occur on the subatomic scale, these are not considered as they are of negligible relevance in the scope of organic coating adhesion for corrosion protection. For this reason, the most fundamental interactions that will be discussed are those at the intermolecular scale.

1. **Interactions through electron pair sharing** These interactions constitute chemical bonding of which there are two kinds: ***covalent bonding*** and ***donor-acceptor interactions***. Covalent bonding involves the sharing of one or more electron pairs between atoms. Covalent bonds are short range interactions which operate over distances of the scale of interatomic separations (0.1 - 0.2 nm). A donor-acceptor interaction is the instance where one or more electrons are removed (donated) from one atom and attached to another such that a positive and a negative ion are from which are attracted to each other.

2. **Electrostatic interactions** Also known as the Coulomb force, this occurs between charged particles where interaction take place according to Coulomb's law which quantifies the attraction and repulsion between said particles:
$$F = k\frac{q_1 q_2}{4\pi\epsilon r} \tag{3.3}$$
where
$q_{1,2}$ are the charges on each of two interacting charged particles

ϵ is the dielectric constant of the medium containing the charged particles and
r is the distance between the charged particles.

3. **van der Waals interactions** These are interactions dependent on the distance between atoms or molecules.

   Dipole-dipole interactions. Some atoms draw electrons more strongly to themselves than others. This ability is dependent on the electronegativity of that atom. The more electronegative an atom is, the more strongly it attracts electrons to itself. Therefore, in a molecule, where there is an atom or group of atoms on one end of the molecule that possesses a higher electronegativity, a partial charge is created on either end of the molecule. These partial charges are capable of attracting other oppositely charged or partially charged species and repelling like charged species.

   Dipole-induced dipole. Electrons exist according to a probability distribution in molecular orbitals around nuclei. These orbitals are capable of interacting either charges including the partial ones of a dipole. Even a molecule with a symmetrical charge distribution upon interaction with a dipole would have its electrons attracted to the positively charged end of the dipole and repelled from the negative end. In this way, the initially symmetrical charged distribution is skewed and a dipole is induced.

   Dispersive forces These forces, unlike dipole-dipole interactions and induction forces, involve the simultaneous excitation of the two atoms/molecules participating in the interaction. These forces are always present between particles within sufficient proximity. They exist as a result of the constant fluctuation of electrons relative to the positively charged nucleus. This fluctuation generates an electrical field around the particle that polarizes the neighbouring particle. This happens in both interacting species and therefore results in an instantaneous attractive force which is referred to as the dispersive force. In contrast to the other two van der Waals interactions described above, this type of interaction is nonpolar [31, 32].

Adhesion may be quantified thermodynamically by way of the work of adhesion. It is so called because it is based on the concept of free energy, etc, etc.

3.5 Adhesion failure mechanisms

According to Dickie [29], the following are the various mechanisms by which failure of organic coatings on galvanized steel may occur:

- Water disruption of interface
- cathodic alkali disruption of the interface
- cathodic alkali degradation of the interface
- cathodic alkali degradation of the coating polymer
- cathodic alkali degradation of the substrate

The literature suggests that, in any particular case of coating adhesion loss, it is usually due to more than one of the aforementioned mechanisms simultaneously coming into play to ultimately cause adhesion failure. Overall, it appears to be the case that should the cathodic reaction be inhibited, the majority of these failure mechanisms would be hindered.

3.6 Polymer additives for adhesion enhancement

Polymer additives in conversion solutions are incorporated for the purpose of improving the adhesion of organic coatings to the conversion layer. This practice dates back to early chromium pretreatments where polyacrylic acid (PAA, Figure 3.2a) was incorporated in the conversion bath having been found to increase corrosion resistance [1, 33].

Deck et al. [34] studied the effect of PAA, as an additive in fluoacid conversion baths, had on the surface chemistry of Al. Addition of PAA in general, improved coating properties. Results of Deck's investigation suggested that this was due to the formation of a polymer film on the Ti/Zr oxides. It was found, however, that Zr is more effective in this regard than Ti. This is because Zr is able to act as a cross-linking agent while Ti does not possess the same capability.

Polyvinyl alcohol (PVA, Figure 3.2b) was found in some patents to provide additional corrosion protection and coating adhesion strength when employed in combination with PAA [35, 36]. The two polymers crosslink by forming an ester linkage. The film formed via this process provides further protection for the substrate from ion-exchange.

Another polymer additive encountered in the literature is polyvinyl pyrrolidone (PVP, Figure 3.2c). It is reported to increase corrosion resistance of the surface and also the wettability of the treatment solution for galvanized steels [37]. It is also employed as a dispersant in zinc phosphate conversion solutions [38].

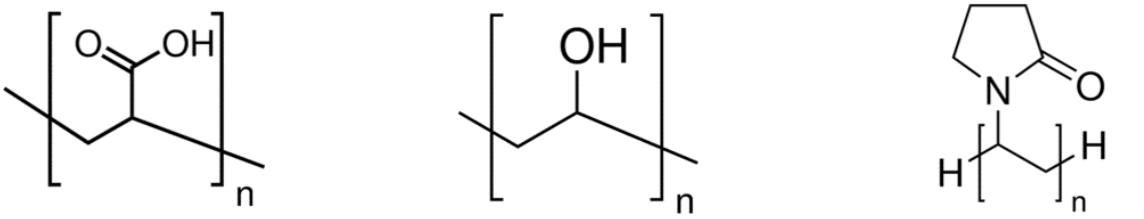

(a) Polyacrylic acid **(b)** Polyvinyl alcohol **(c)** Polyvinyl pyrrolidone

Figure 3.2: Organic additives studied in this research

3.7 Quantification of adhesion strength

There are three primary types of mechanical tests performed to evaluate adhesion in general. The difference in test type lies in the way in which the adhesive bond is loaded in each. The loading types are as follows:

1. Tensile loading

   In tensile testing, the coating-substrate system is subjected to stress normal to the plane of adhesion over a specific cross-sectional area. This method of testing has the advantage of being straightforward to perform and also more quantitative compared to other adhesion test methods. The quantitiy measured is the amount of energy required to remove

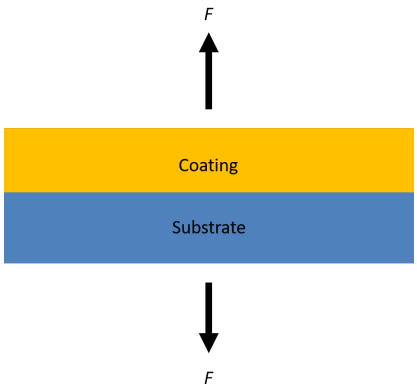

Figure 3.3: A coating-substrate system to which a tensile force is applied. The area subjected to the force should be known for accurate characterization of adhesion

2. Shear loading
   Many test methods are based on shear loading. The highest adhesion strengths are displaced when an adhesive bond is loaded in shear.

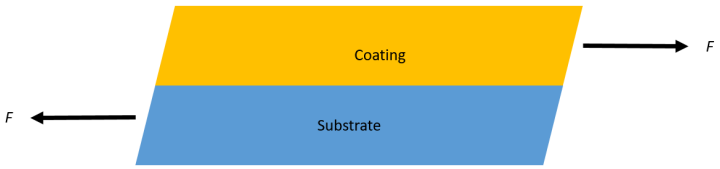

Figure 3.4: A coating-substrate system loaded in shear

3. Cleavage loading
   Cleavage loading, as illustrated below in Figure 3.5, is one of the most severe forms of stress to which an adhesive bond may be subjected. Tests employing this mode of loading may also be referred to as peel tests.This class of tests are better suited to thicker coatings as thin coatings are more susceptible to breaking before adhesion between the coating and substrate fails.

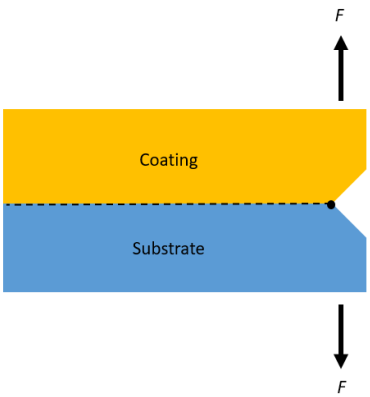

Figure 3.5: A coating-substrate system under cleavage loading

Chapter 4

Corrosion protection of galvanized steel: Corrosion inhibitors

Inhibition refers to corrosion prevention by adding substances which significantly retard corrosion of a surface when added in small amounts to otherwise corrosive environments [39, 40]. Selection of inhibitors for any application is based on their solubility in the fluid surrounding the substrate to be protected and can be organic or inorganic. In general, inhibitor pigments prevent corrosion by slowing down or completely hindering either the cathodic or anodic corrosion reactions or both by obstruction the movement of the requisite ions as shown below in Figure 4.1.

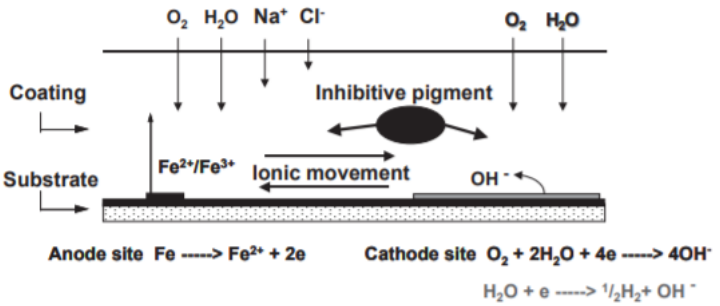

Figure 4.1: Inhibition mechanism of inhibitive pigments [39]

Corrosion inhibitors may be classified according to their effect on the anodic and cathodic reactions involved in corrosion:

- Anodic inhibitors
- Cathodic inhibitors
- Mixed inhibitors

Inhibitors may be either anodic or cathodic depending on which of the relevant corrosion reactions they impact. Anodic inhibitors usually work by forming an oxide layer on the surface of the metal. This causes an anodic shift of the corrosion potential towards the passivation region. Consider the anodic reaction:

$$\mathrm{M} \longrightarrow \mathrm{M}^{n+} + ne^{-} \tag{4.1}$$

Requirements of an inhibitor for galvanized steel studies estimate that the demand for corrosion inhibitors in the US alone rises by 4.1% every year. Currently, the focus in the field is on environmentally friendly corrosion inhibitors. Some researchers have looked into natural products such as essential oils, plant extracts and other biological products as possible replacement for chromate active inhibitors. Drugs have also been studied as corrosion inhibitors as well other metal compounds like molybdates and cerium compounds.

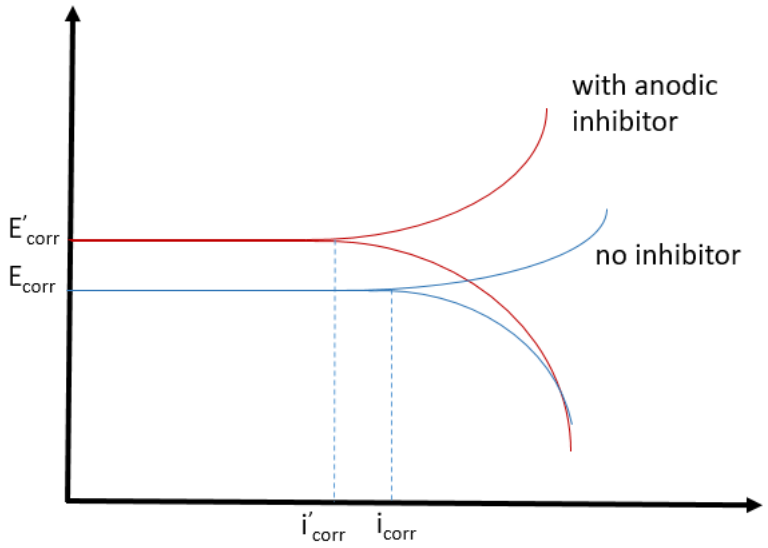

Figure 4.2: Potentiostatic polarization diagram showing the electrochemical behaviour of a metal in an electrolyte in the presence and absence of an anodic inhibitor

Inhibitors can therefore be classified by whether they are biological or synthetic products. A further distinction can also be made based on their inhibitive mechanism .

Anodic inhibitors are also called passivation inhibitors. A graphical illustration of anodic inhibition is found when one compares the polarization curves of a metal in a corrosive electrolyte without inhibitors and of one with anodic inhibitors. An example is shown below in Figure4.2.

Metal ions produced during anodic dissolution react with anodic inhibitors to produce metal hydroxides and/or oxides which are deposited on the metal surface to form an insoluble protective layer. At sufficient concentrations of anodic inhibitors, the rate of passivation which generates higher cathodic current density, exceeds the rate of the anodic reaction. This favors the formation of the passivation film and the corrosion potential is shifted to a more noble value. In this way, anodic dissolution is significantly reduced or prevented entirely and the metal surface is passivated[41, 42]. As shown in Figure 4.3,the corrosion potential and current density are reduced by adding an anodic inhibitor.

Cathodic inhibitors produce insoluble species which selectively deposit on cathodic sites thus, suppressing the cathodic half of the corrosion reaction. This lowers the equilibrium potential and decreases the current density.

There are three main ways by which corrosion inhibition is achieved. These are by:

1. Passivation
   As explained in Chapter 2, passivation involves the formation of a film that is insoluble in the surrounding electrolyte which is able to prevent or significantly reduce the corrosion of a metal. Many inhibitors are able to enhance the corrosion prevention capability as well as the speed of film formation once breach of the coating system occurs. Inhibitors such as silicates, carbonates and phosphates are able to maintain a slightly alkaline pH near the metal surface which helps to prevent dissolution [43].

2. Precipitation of compounds
   These compounds whose precipitation at the surface layer forms a layer that reduces the rate of

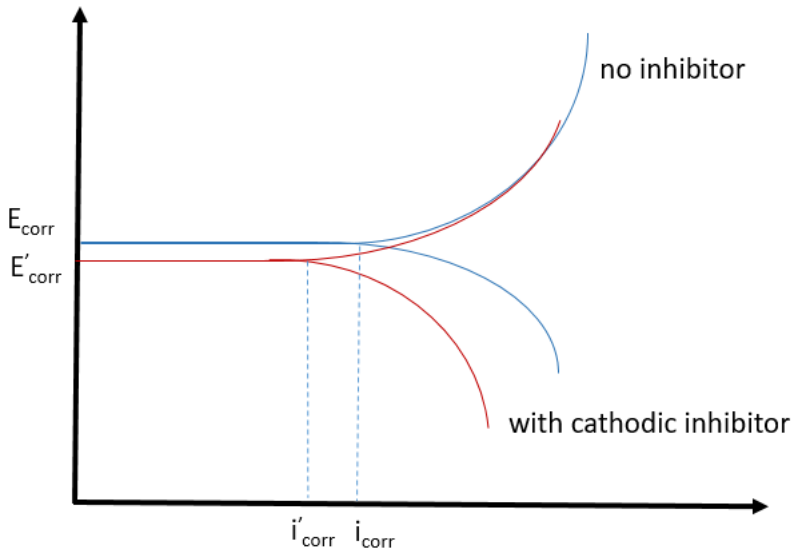

Figure 4.3: Potentiostatic polarization diagram showing the electrochemical behaviour of a metal in an electrolyte in the presence and absence of a cathodic inhibitor

metal ions away from the metal after dissolution and in the same way, that of electrolyte species to the metal .

3. Adsorption
   This type of inhibition involves adsorbates usually organic compounds, with high electron densities at the head group which binds the molecule to the substrate. The long organic chains attached to the head groups provide physical coverage of the surface which slows down the migration of species from the bulk electrolyte to the surface and vice versa.

4.1 Polyphosphates

Polyphosphates are favored corrosion inhibitors especially for application in cooling water systems. For instance, it was found that on mild steel in natural water, inclusion of polyphophates in the form of metaphosphate glass leads to the formation of a protective film consisting of iron, calcium and phosphate[24, 44]. The presence of calcium in the film composition is explained by the fact that the use of polyphosphate inhibitors requires the presence of divalent/polyvalent ion eg. calcium, magnesium, to provide sufficient protection[44, 45]. In the absence of added cations, polyphosphates will form a complex with the metal cations formed by the corrosion process to form a protective film at the surface.

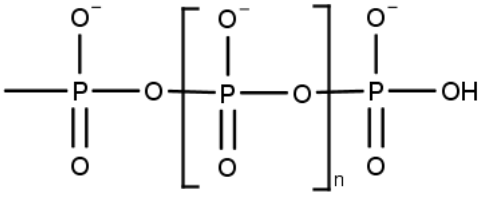

Figure 4.4: Polyphosphate structure

The argument for the use of polyphosphates as corrosion inhibitors cites a number of points some which of which include the requirement of small amounts of the material to achieve adequate protection, its solubility in water and an ability to form a barrier film via electrodeposition.

4.2 Calcium ion exchange

The inhibitive effect of Ca was studied by Zen et al. [46] in calcium modified zinc-phosphate coatings on steel. Zin et al. [47] also established in a highly cited paper that when zinc phosphate and calcium exchanged silica are combined, a synergistic effect occurs which significantly inhibits corrosion galvanized steel. As an inhibitive pigment, calcium is commonly manufactured and sold in the form of calcium exchange silica. It is widely accepted that the means by which these pigments inhibit corrosion is via an ion exchange mechanism. The calcium ions are released by exchange with cations in the solution and followed by further dissolution of the pigment which releases polysilicate ions. The silicate and calcium ions deposit on the surface and this way form a layer which prevents aggressive species (eg. H^+ and Cl^-) from reaching the surface [48, 49].

Chapter 5

Materials and Methods

5.1 Materials

Both MagiZinc(MZ) and hot-dip galvanized steel (GI) steel were sourced from Tata Steel as 300 × 200 mm sheets with thickness 0.4 mm. The GI steel surface consists of zinc layer with 1% Al. The MagiZinc surface comprises Zn - 1.6% Al - 1.6% Mg. Both GI and MZ as received had a thin organic layer at the surface which was applied by the manufacturer to protect the surface. For alkaline cleaning 1 M NaOH was prepared and adjusted to pH 12 using phosphoric acid.

Hexafluorozirconic acid and hexafluorotitanic acid were the reference conversion solutions for the investigation of the effect on coating adhesion of polymer additives. This choice was based on their established effectiveness in this regard. These were each prepared at a concentration of 0.01 M and adjusted to pH 4 using 1 M NaOH.

The polymer additives investigated as potential adhesion enhancers were polyvinyl alcohol, polyvinylpyrrolidone and polyacrylic acid. A prior screening was conducted using potentiodynamic polarization to ascertain the range of concentration at which it was feasible to test these polymers in the conversion solutions. From this screening test it was established that for some of the polymers there was a minimum threshold below which their effect on the polarization behaviour of the substrate was no longer significant. Based on these results, test concentrations were decided. Table 5.1 below shows the solutions used:

Table 5.1: Composition of tested conversion solutions

Solution	H_2ZrF_6 [M]	H_2TiF_6 [M]	PAA [$g \cdot l^{-1}$]	PVA [$g \cdot l^{-1}$]	PVP [$g \cdot l^{-1}$]
Reference	-	-	-	-	-
1	0.01	-	-	-	-
2	0.01	-	0.1	-	-
3	0.01	-	-	0.1	-
4	0.01	-	-	-	0.1
5	-	0.01	-	-	-
6	-	0.01	0.1	-	-
7	-	0.01	-	0.1	-
8	-	0.01	-	-	0.1

To dissolve the polymers, stirring at elevated temperatures was required. PVA and PAA were fully dissolved after stirring for 30 minutes at 70 ℃. PVP required higher temperature and longer stirring time were required. Dissolution was achieved after stirring overnight for about 12 hours at 80 ℃.

The corrosion inhibitors investigated in this study were Hybrocor 206 from WFC Technologies (referred

to as Inhibitor 1 (Inh 1), Novinox ACE 110 (Inhibitor 2) and Novinox XCAO2(Inhibitor 3) from Société Nouvelle des Couleurs Zinciques - SNCZ and Zinc Phosphate ZP10(Inhibitor 7) from Heubach. Hybricor 206 is based primarily on silicates and calcium oxide while Novinox ACE 110 is based on silicates and polyphosphates. Novinox ZCAO2 also has as its primary ingredients, silicates and calcium oxide. The composition of ZP10 comprises primarily zinc phosphate. Each of these inhibitors were incorporated each at two different concentrations in the electrolyte which for this study was 0.05 MNaCl. The composition of each electrolyte tested is shown below in table 5.2.The inhibitors were each incorporated at the concentrations specified in 0.05 M NaCl by stirring at room temperature.

Table 5.2: Composition of inhibited electrolyte solutions tested

Solution	Inhibitor	Concentration [M]
Reference	-	-
1	Inh 1	1×10^{-4}
2	Inh 1	5×10^{-4}
3	Inh 2	1×10^{-4}
4	Inh 2	5×10^{-4}
5	Inh 3	1×10^{-4}
6	Inh 3	5×10^{-4}
7	Inh 2+3	5×10^{-4}
8	Inh 7	2×10^{-5}

5.1.1 Sample preparation

Adhesion test samples

Both GI and MZ sheets were cut into sizes of 50 × 50 mm. Each sample was first cleaned with organic solvents to remove dust and grime from the manufacturing process and from storage. They were rinsed, first in acetone for 10 minutes in an ultrasonic bath and then in ethanol for 10 minutes also in an ultrasonic bath. Then, the samples were rinsed with demi-water and dried with compressed air. The samples were then cleaned in an alkaline 1M of NaOH pH 12 in which they were immersed for 30 seconds. For GI steel, alkaline cleaning was done at an elevated temperature of 60 ℃ to remove the Al layer that diffuses to the surface after hot-dip galvanizing.

The pretreated samples were coated with a model polyester clearcoat from AkzoNobel BV by spin-coating at a speed of 1250 rpm for period of 40 seconds. The samples were then cured in an oven at 225 ℃for 5 minutes. The dry film thickness was then measured using an Elcometer® 456 coating thickness gauge. The device was first calibrated using an uncoated sample of MagiZinc® and GI steel each using the 'zero' calibration method which is ideal for calibrating on uncoated smooth surfaces. The average thickness achieved was 10 µm ± 2 µm.

Corrosion inhibition test samples

Samples were cut into sizes of 40 × 30 mm. Each sample was rinsed in acetone 5 minutes, rinsed with demi-water and then dried with compressed air. Alkaline cleaning was performed similar to the adhesion test in 1 M. A circular area with diameter 16 mm was isolated for electrochemical testing by covering the rest of the sample with impermeable green tape in which a hole of said size had been made. A small section of the sample was left bare at one end where it was clamped to facilitate current flow.

5.2 Methods

5.2.1 Surface analysis techniques

X-ray Photoelectron Spectroscopy (XPS)

The surface composition of MagiZinc and GI were each analyzed both before and after pretreatment using x-ray photoelectron spectroscopy. High-resolution XPS spectra were collected using a PHI5600 photoelectron spectrometer (Physical Electronics) with an Al Kα monochromatic X-ray source (1486.71 eV of photons). The vacuum in the analysis chamber was approximately 8 $\times 10^{-}9$ Torr during measurements. High-resolution scans of the Zn 2p, Al 2p, Mg 2p, Zr 3d, O 1s, C 1s, and F 1s XPS peaks were recorded from a spot diameter of 0.8 mm using pass energy of 23.5 eV and step size 0.1 eV. Measurements were performed with take-off angles of 45° with respect to the sample surface. The reproducibility was verified by triplication of the measurements. XPS data was analyzed with PHI Multipak software (V9.1.0.9). Before curve fitting, the energy scale of the XPS spectra was calibrated relative to the binding energy of adventitious hydrocarbons (C C/C H) in the C 1 s peak at 284.8 eV. Curve fitting was done after a Shirley-type background removal, using mixed Gaussian-Lorentzian shapes. XPS allows the identification of changes to the atomic composition of the surface caused by the various pretreatments.

ATR/FTIR

FTIR measurements were carried out on a Thermo-Nicolet Nexus equipped with a liquid-nitrogen cooled mercury-cadmium-telluride (MCT) detector and a nitrogen-purged measurement chamber with a Veemax III single reflection ATR accessory.Depth profiling studies were conducted using germanium ATR-crystals at variable set angles of incidence. The ATR-crystals (PIKE Technologies) had a fixed face angle of 60°. 50 nm zinc (Goodfellow, 99.95%) was deposited on the ATR crystals by means of a high-vacuum evaporation system (VCM 600 Standard Vacuum Thermal Evaporator, Norm Electronics). A polymer coating with polyester-based resin, Dynapol LH 820 (Evonik Industries AG) was applied using a 30 Âţm bar coater. The resulting polymer film was cured for 15 minutes at 130 ℃. Infrared backgrounds were obtained from the ATR-crystals with and without zinc film before the application of the polymer coating. Infrared spectra were averaged for 128 cycles with a resolution of 4 cm^{-1} and were normalized to the background spectrum. The control of the spectra acquisition and incident angles was managed by the OMNIC 8.1 software package (ThermoElectron Corporation, Madison, WI). FTIR provides detailed molecular information about changes to interfacial chemistry due to the different pretreatments. It is, as such, instrumental in determining the nature of the chemical bonds involved in coating adhesion.

Atomic Force Microscopy (AFM)

Roughness was measured on a representative 100 µm × 100 µm area. This was to determine the effect of the various additives on the roughness of the surface. From this, the correlation between roughness and adhesion could be investigated.Surface roughness was measured with the Atomic Force Microscope (AFM) Dimension Edge Scanning Probe Microscope from Brujker.

Contact Angle Measurements

Surface energy of the sample surfaces was measured using a OneAttension optical tensiometer. MilliQ (ultrapure water of Type 1), ethylene glycol and diiodomethane were the liquids using in measuring. The procedure involved placing a drop of liquid with volume 1.5 1.5 µl on the surface of the sample and then measuring the contact angle at the metal-liquid-air interface from the moment of liquid contact until the angle reached a stable value. From this test the dispersive and polar contributions to the work of adhesion were measured. Using the following equation, it was then possible to calculate the work of adhesion.

Pull-off adhesion test

To quantify adhesion, the pull-off adhesion test, according to the ASTM D4541-17 standard (Figure 5.1, was performed. While this test method does not truly reflect the usual way in which adhesion loss occurs on galvanized steel in actual application, it can be used to obtain 'a figure of merit' for the strength of coating adhesion to the substrate. To perform the test, dolly of 20 mm diameter was then attached to each sample using the SG300-05 adhesive from SciGrip.. These were left to cure at room temperature, after which the dollies were pulled off at a rate of 10 mPa per second using the Elcometer 106 Pull-Off Adhesion tester.

Due to the low thickness of the samples, prior to testing each sample was glued to a 4 mm thick steel substrate to prevent bending. The glue used was a cyanoacrylate chosen for its stiffness and strength. Additionally, prior to testing, the coating was cut around the dolly to prevent applying any shear stresses to the bond between the dolly and the coating as this would increase the chances of bond failure and render measurements inaccurate. To further prevent such an occurrence, a clamp was devised which comprised two slaps of thick, stiff plastic, in one of which was drilled of the diameter of the dolly cutter. This was to clamp the coated sample with the attached dolly such that it did not shift during cutting and also so that dolly did not move the dolly in the process. It has been shown that in fact, when there are no measures take to prevent shear stress like in this study where the coating was cut before the dolly was attached pull-off values were 14% lower than with these preventative measures in place.

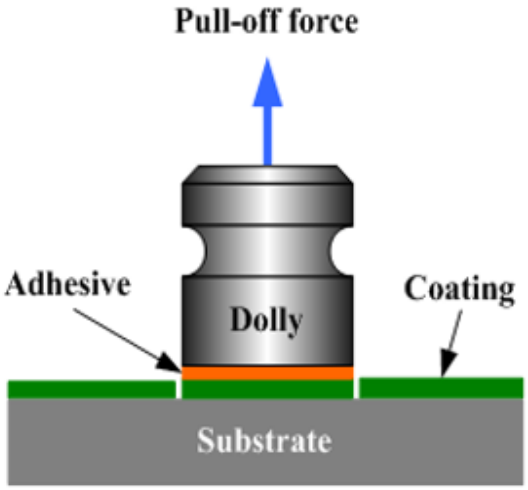

Figure 5.1: Pull-off adhesion test

5.2.2 Electrochemical analysis techniques

Potentiodynamic Polarization

Potentiodynamic polarization tests were performed to determine the influence of each inhibitor on the electrochemical reaction kinetics of MagiZinc. Two samples each were used for each test. Anodic polarization was conducted on sample starting at -0.3 V relative to OCP and then scanning up to 0.5 V relative to OCP. The OCP was established from OCP measurements. The cathodic polarization was carried out on the second sample from 0.03 V to -0.5 V versus OCP. An overlap region between -0.03 to 0.5 V versus OCP was necessary to facilitate further processing of the data. A Tafel extrapolation of data was done to determine i_{corr} and E_{corr}.

Linear Polarization Resistance

LPR is used to gain information about the resistance of a sample to polarization. In this test, the sample is polarized in both the anodic and cathodic directions relative to the open-circuit potential (OCP). A current is induced while potential is varied. The slope of the potential versus current plot gives the material's resistance to corrosion. In this study, LPR tests were conducted on a VSP-300 potentiostat from BioLogic Scientific Instruments SAS. The potential was varied at a rate of $0.167\,\mathrm{mV\,s^{-1}}$ from an initial potential of $-5\,\mathrm{mV}$ relative to OCP to a final value of $5\,\mathrm{mV}$ relative to OCP. Current was recorded every 0.1 with the value of the current recorded at each step being the average over 5 voltage steps of the current values measured during the last 25% of the step duration. Each measurement took a minute in total. LPR measurements were recorded every hour for 168 hours.

Electrochemical Impedance Spectroscopy

Impedance measurements were performed on MagiZinc samples in each of the inhibitors, each at a concentration of 0.5 mM as well as in a reference electrolyte of NaCl at 0.05 M concentration. These measurements were performed to determine the point at which the electrochemical system became stable. Measurements were carried out on the BioLogic VSP-300 in sine mode. The sample was left to reach OCP for 15 minutes and 40 seconds which served as the starting potential for impedance measurements. Scanning was from an initial frequency of 100 kHz to a final frequency of 10 mHz. Eight points were recorded per decade. These two techniques were repeated consecutively in a loop 168 times (7 days).

Chapter 6

Results and discussion

6.1 Effects of polymer additives in chromium-free pretreatments on organic coating adhesion

The first results addressed in this chapter are those of the pull-off adhesion tests. Subsequently, the results of the various surface characterization tests are presented. Significant correlations, trends and general observations concerning the surface characterization results are then expanded on. Electrochemical analysis of the sample surfaces will thereafter be presented and the implications for corrosion behaviour will be discussed. The last part of this chapter will be a discussion of the results of the electrochemical analysis data from testing of the various corrosion inhibitors.

6.1.1 Pull-off adhesion strength

Figure 6.1 shows the pull-off adhesion results on GI for the various pretreatments tested.These values represent the magnitude of the tensile loading at which detachment of the dolly from the coated sample occurred (see Fig 5.1). Pretreatment with H_2TiF_6 and H_2ZrF_6 without the inclusion of a polymer additive results in an increase in the strength of adhesion between the organic coating and the substrate. The failure stress increases from 7.3 MPa to 8.6 MPa when theh surface is treated with H_2TiF_6. An even further increase in adhesion strength is achieved when treated with H_2ZrF_6 with a pull-off adhesion strength value of 9.4 MPa.

The addition of polymer additives to the conversion solution however produces an interesting result. The inclusion of these additives appears to be detrimental to coating adhesion on GI. All three additives tested resulted in a decrease of the strength of adhesion of the coating to the GI samples. The lowest adhesion values were observed on samples pretreated with Ti-based conversion solutions. In combination with polymer additives, Ti pretreatments result in adhesion strengths that are even lower than that of the untreated surface. For GI, it appears treatment with Ti/Zr pretreatments is sufficient for adhesion improvement.

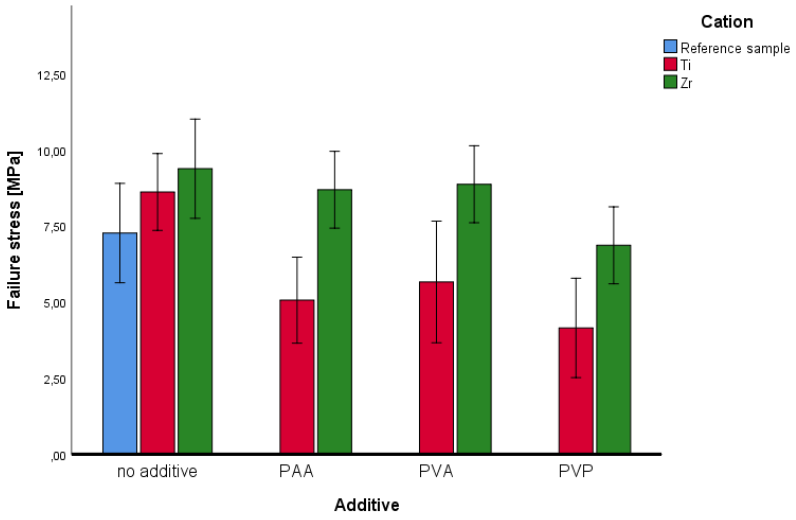

Figure 6.1: Pull-off adhesion strength of polyester coating to GI as a function of polymer additive type present at coating-substrate interface

The results of pull-off adhesion testing on the second galvanized steel type, MagiZinc are shown in Figure 6.2 below. Similar to the results for GI, pretreatment with H_2TiF_6 and H_2ZrF_6 without the inclusion of a polymer additive results in an increase in the strength of adhesion between the organic coating and the substrate. However, significant departures from the trends identified for GI were observed in the tests conducted on MZ. The most visible difference is that the Ti-based treatments result in a larger extent of adhesion improvement than the Zr treatments. The adhesion failure stress on samples treated with H_2TiF_6 increases from 4.4 MPa to 7.2 MPa as a compared to the untreated state. The H_2ZrF_6 pretreatment results in an increase to a lower final adhesion strength of 5.7 MPa.

Furthermore, with the inclusion of additives, dissimilar to GI, the adhesion strength of MZ is increased in all cases. The PVP additive results in the largest adhesion improvement with a stress of 11.2 MPa required to detach the coating from the metal surface.

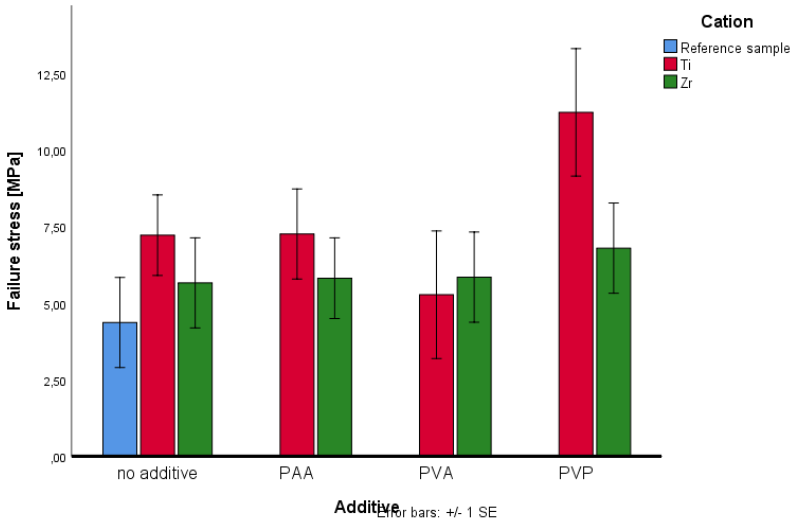

Figure 6.2: Pull-off adhesion strength of polyester coating to MagiZinc® as a function of polymer additive type present at coating-substrate interface

6.1.2 Surface elemental composition

The adhesion test results discussed above give an indication of the variation in coating adhesion performance as a function of the type of pretreatment employed for a particular substrate. For a fuller and more nuanced picture, it is necessary to understand the specific parameters, both chemical and physical, at the interface that are affected by changing the cation in the hexafluoro- compound and/or the polymer additive in the conversion solution and how these in turn affect coating adhesion. For this purpose, various surface analysis studies were conducted.

The first set presented in this chapter are those from XPS analysis and are shown below in Figure 6.3. These give an indication of the extent of conversion that occurs on a given substrate after immersion in the conversion solution. The parameter probed is the relative amount of each surface group present at the surface and how this is changed by a particular surface treatment. From these results, we will investigate whether or not this parameter has a significant influence on adhesion by comparing the results from this test to the adhesion results as well as the other surface analysis techniques conducted.

In Figure 6.3, the percentage of the initial components: Zn (blue), Mg(red) and Al(green) were measured on both treated and untreated samples of GI (Figure 6.3a) and MagiZinc (Figure 6.3b) are represented. For GI, the pretreatment solution based on Zr resulted in a much higher reduction of the relative zinc content as compared to the Ti pretreatment which yielded a decrease to 20.6%. The Zr pretreatment lead to a component percentage decrease of Zn from 28% to 6%. The relative Al component after the pretreatments reduced to from 0.8% and 0.9% for the Ti and Zr pretreatments respectively from 7.2% as shown in 6.3a.

As represented in Figure 6.3b, on MagiZinc®, an interesting trend is observed. Rather than decreasing after pretreatment as observed for GI, the relative Zn percentage increases from 4.5% to 15% after pretreatment with H_2TiF_6. The proportion of MG and Al are also significantly reduced after this treatment from 3.5% to 0.6% and from 2.6% to 0.4% respectively. It is apparent from the measurements of atomic composition that when an H_2TiF_6 solution is used to treat MagiZinc, the Mg and Al-rich phases are preferentially dissolved (Figure 6.3b). This indicates that the effects of any individual pretreatment would be dependent on the elemental composition of the surface being treated.These results are confirmed by the study by Lostak et al. [50] which proposes that the deposition of Zr on Zn-Mg-Al surfaces starts with the anodic dissolution of Al and Mg and preferential deposition on local Zn-rich cathodes.

After treatment with H_2ZrF_6, the relative composition of Zn of MZ is decreased from 4.5% to 1.4% , for Al from 3.95% to 0.5% and for Mg from 2.6% to 1.6%. The relative composition of OH groups at the surface appears to have no bearing on the strength of coating adhesion. The cation component appears to play a dominant role here instead. For instance on GI, the Zr treatment results in a higher relative Zr atom component on the surface and it is for this same Zr treat that we observe the highest coating adhesion values. The same is true for MZ, the highest relative pretreatment cation composition is achieved with Ti and this is mirrored in the coating adhesion tests in which Ti-pretreatments exhibit higher adhesion strength.

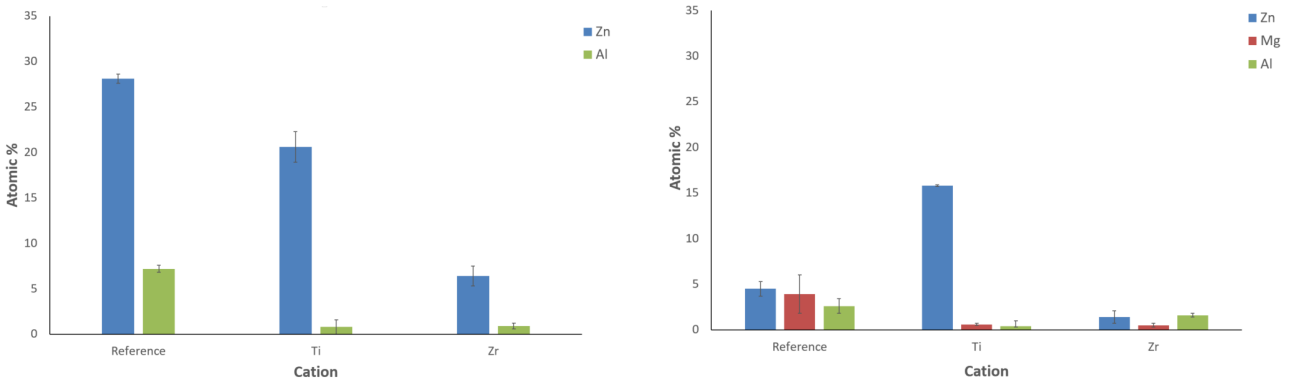

(a) Hot-dip galvanized steel **(b)** MagiZinc®

Figure 6.3: Atomic composition of MagiZinc® and GI surfaces before and after pretreatment

The relative composition of hydroxyl groups and cations at the surface both before and after pretreatment was investigated. This was done in order to give an idea if these effects would influence the final adhesion results. Figure 6.4, shows this comparison. In both cases and for all treatments, the percentage of OH remains higher than that of the cation. On the hot-dip galvanized steel, the relative amount of OH reduces from 56% at the surface to 28% for the Ti treatment and to 31% for the Zr treatment while 10% of the surface is taken up by Ti atoms. MagiZinc on the other hand, displays the reverse trend with respect to the various pretreatmnet cations on the relative amount of OH present on the surface. We find that the pretreatment with Ti cations results in a substantial reduction of OH ions on the surface from 77% to 19% while for Zr, the reduction is slightly less pronounced with a value of 23%.

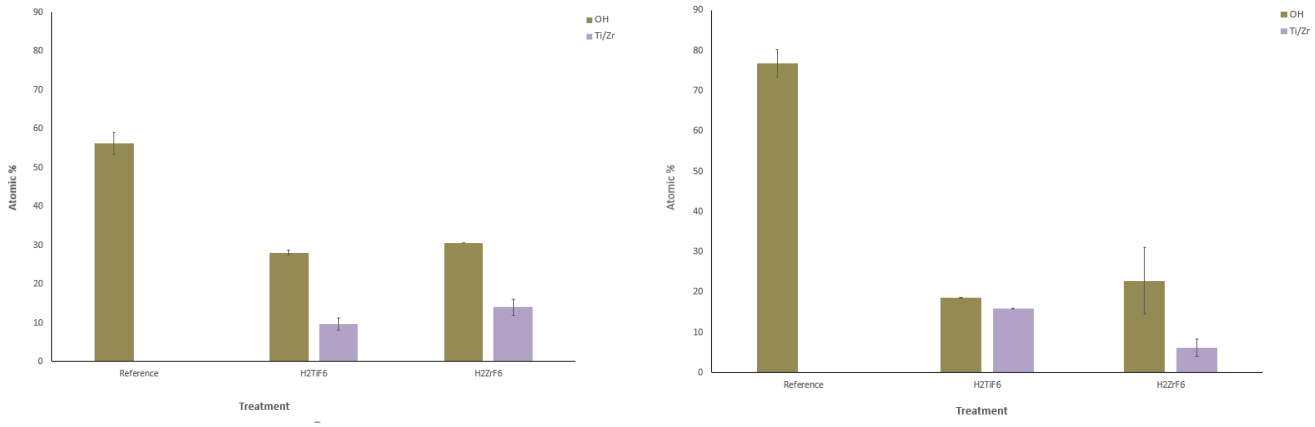

(a) GI **(b)** MagiZinc®

Figure 6.4: OH and conversion cation composition omn MagiZinc® and GI surfaces before and after pretreatment

Surface contaminants exist on most surfaces and differ based on the history of the sample. Minerals in the water used in rinsing at the plant, oils, dust and grime from the fabrication process, and contaminants produced by stray currents during electrochemical processes could all play a role. These contaminants have an effect on coating adhesion and may become initiation points for corrosion. To exclude these effects on coating adhesion and electrochemical behaviour, the amount of contamination present on the surface and therefore the extent of its influence on the behaviour observed should be identified. The initial and final thicknesses of the contamination layer on each surface were thus measured to ascertain how the various treatments affected the extent and to be able to account for these effects in the electrochemical and adhesion results. Characterization of this layer is possible through infrared spectroscopy due the fact

that many of the component substances, namely hydrocarbons and silicones, exhibit mid-IR transmission spectral signatures [51]. A typical IR spectrum of a grease surface contaminant is shown in Appendix B.

The contamination layer thicknesses measured on MZ and GI pretreated with H_2ZrF_6 and H_TiF_6 are shown below in Figure 6.5. The thicknesses measured on hot-dip galvanized steel substrates are represented by the purple bars while those for MagiZinc® are shown in red. It is apparent from this graph that neither pretreatment significantly changes the thickness of the contamination layer on the hot-dip galvanized steel substrate. However, it is important to note that the initial thickness on the GI surface to begin with is very low at 5 nm. The contamination layer on the MagiZinc substrate, on the other hand, is significantly reduced after immersion in the H_2TiF_6 solution from 20 nm to 3 nm. The zirconic acid treatment on the other hand, yields no significant difference in the thickness 6.5 as compared to the reference.

The effectiveness of the titanium treatment at reducing the contamination layer on MagiZinc could also be a possible contributor to the relative zinc content on this substrate being so significantly increased after the treatment.

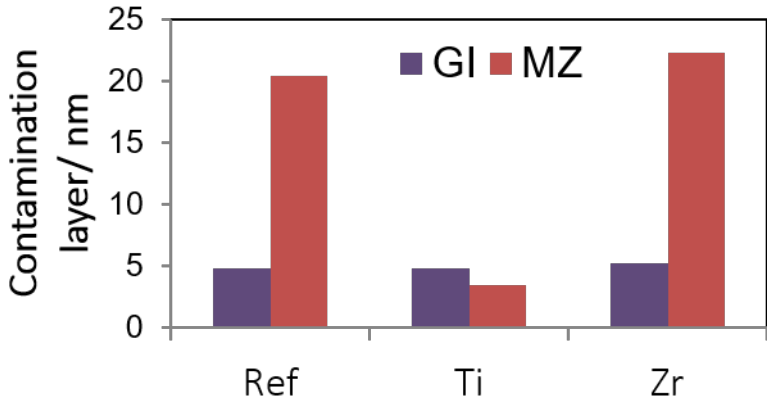

Figure 6.5: Thickness of contamination layer after pretreatment

6.1.3 Chemical interactions at the coating-metal interface

It is generally accepted that adhesion is the sum of both chemical and physical interactions. However, many argue that chemical interactions are the predominant determinant of adhesion and adhesive performance. It appears that these effects are dependent on the substrate-coating system in question. In this project both interactions were investigated. ATR-FTIR measurements show that chemical bonding is primarily based on bonding between carboxylate groups in the polyester coating and oxide and hydroxyl groups on the metal surface.

Figure 6.7 below shows the interfacial stability as a function of the immersion time in water. We propose a mechanism based on the findings of Pletincx et al to explain the behaviour depicted in this graph. [52]. The first step involves the deprotonation of the carboxylic acid functional groups of the coating by water and the resulting creation of hydroxonium ions. The carboxylate groups formed react with the hydroxyls at the metal surface and hydroxide ions are formed as a result. These, together with the hydroxonium ions produced in the first step of the mechanism, sustains the equilibrium of self-ionization of water. The mechanism is repeated until all the available functional groups on the polymer and/or the

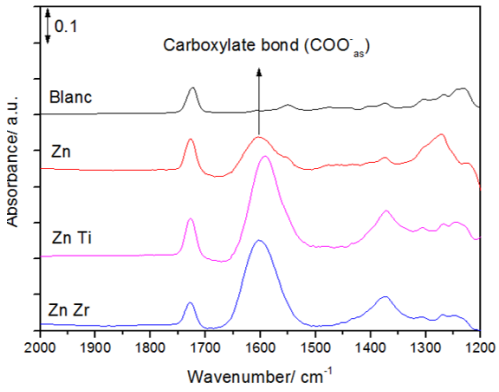

Figure 6.6: Bond formation between organic coating and substrate

metal surface at the interface are reacted. Once this happens, the carboxylate groups detected reaches maximum. After this point, given sufficient humidity, water replaces the ionic bonds formed between the polymer and the metal surface. This accounts for the decline in carboxylate ion groups as observed in Figure 6.7 which is also mirrored by the decline in peak area of OH_. Eventually, the peak area for carboxylate and hydroxyl ions attains negative values due to the fact the measurements were made relative to the polymer-coated metal.

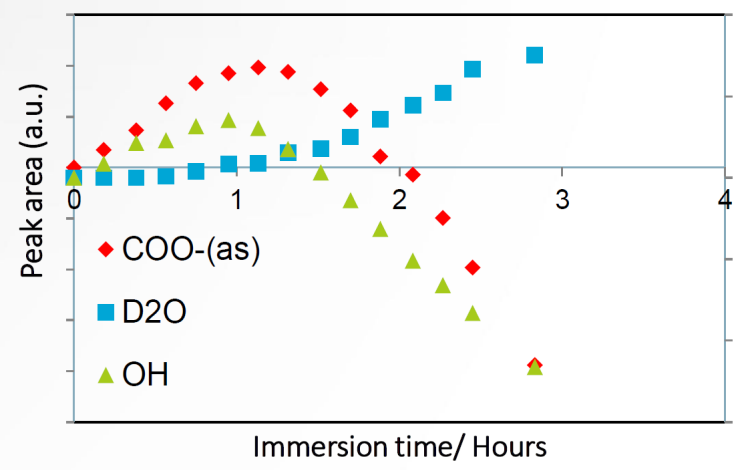

Figure 6.7: IR peak areas of COO^-, D_2O and OH_ at the interface of polyester-coated galvanized steel after exposure to water (D_2O) as a function of time after the commencement of exposure

Based on these results, a conjecture can be made about the bond formation mechanism. The process begins with the hydrolysis of the ester bond which leaves a negatively charged oxygen ion. This attaches either to a hydroxyl group by ionic bonding or replaces a hydroxyl group and bonds to the cation as shown in Figure 6.8.

6.1.4 Surface roughness

Surface roughness has also been suggested as having a significant influence on coating adhesion. This is based on the fact that higher surface roughness increases the surface area available for interactions between the organic coating and the metals surface. The R_q values measured for MagiZinc after the

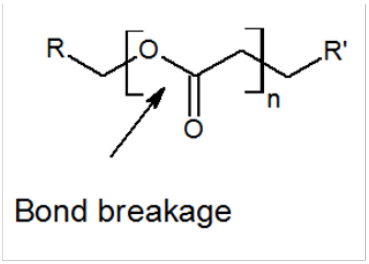

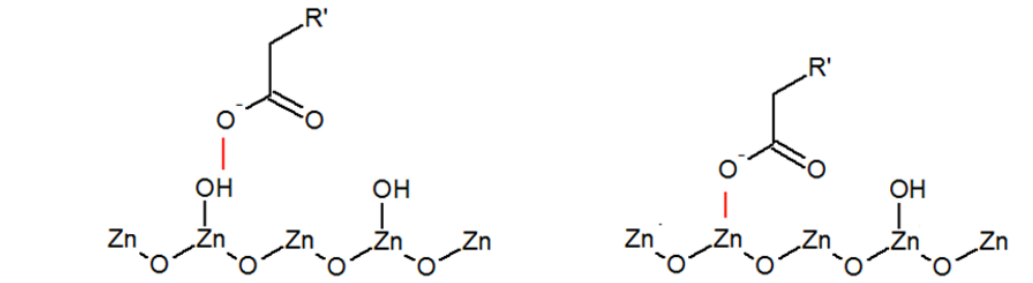

H]

Figure 6.8: Proposed adhesive bond formation mechanism

various pretreaments are shown below in Figure 6.10a and for GI in Figure 6.10b. Uncoated MagiZinc and GI surfaces are used as references. The R_q value is the root mean-squared roughness of the surface which is calculated as follows:

$$R_q = \sqrt{\frac{1}{L}\int \left|Z^2(x)\right| dx} \tag{6.1}$$

where
Z is the height of the surface profile as shown below in figure in and
x is the length along the evaluation length, L.
Due to the squaring of values in calculating R_q, it is more sensitive to peaks and valleys on the surface making it a more indicative measurement than R_a [53].

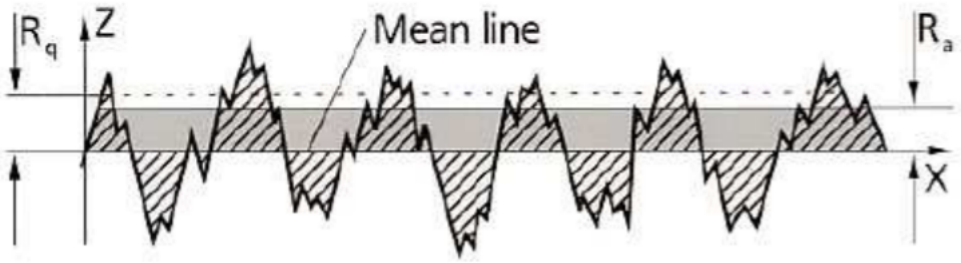

Figure 6.9: A profile of a surface showing the various parameters used to characterize roughness. R_q is the root mean-square roughness, Z is the height of the profile surface (the height from the bulk to the highest point surface at the given point and R_a is the average of all the roughness values measured [53]

It is evident from this graph that for MagiZinc, all pretreatments reduced surface roughness compared to the roughness of untreated samples. The trend was however not identified in the pull-off adhesion results obtained from the experiments as will be shown in a subsequent section. This may be because

as reported by Khun and Frankel [21], above a certain roughness threshold, the positive effect of surface roughness on improving coating adhesion is no longer significant. In Khun and Frankel's study, this threshold was observed at an R_q value of 70 nm. Roughness values observed in this study were much higher with the lowest recorded R_q values being in the range of 300-400 nm. The conclusion therefore is that the Zr/Ti do not increase adhesion by increasing the surface roughness but rather by strengthening the chemical interactions at the interface. The chemical effect is dominant.

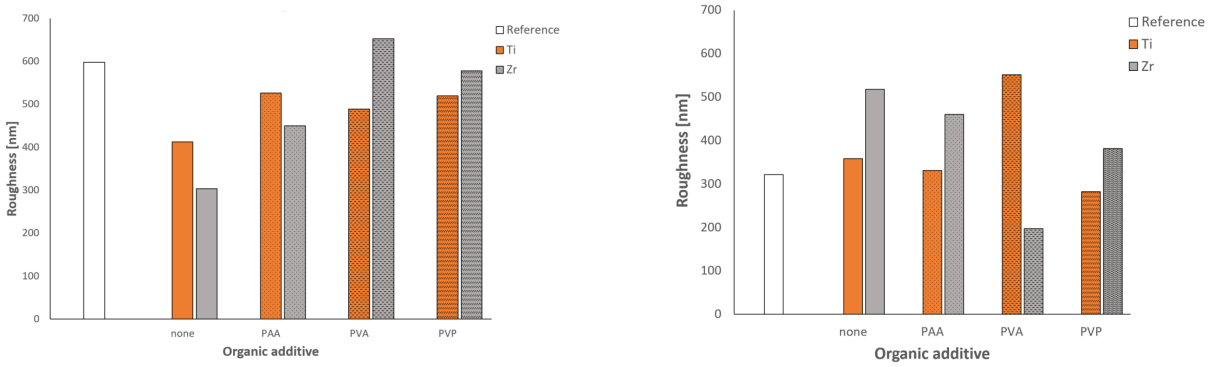

(a) MagiZinc®

(b) GI

Figure 6.10: Effect of organic additives in pretreatments on surface roughness on MagiZinc® and GI

No error bars are included for the roughness measurements due to the fact that these values are the result of an AFM mapping of a representative area of the sample measuring 100 × 100 nm in size.

6.1.5 Surface energy

As mentioned in Chapter 3, one way of quantifying adhesion is by measuring the work of adhesion. This is a quantity derived from the surface energy calculated via contact angle measured between liquids with known surface energy and the surface of interest. The contact angle on each sample was measured as described in the previous chapter. Surface energy was calculated from these values using the Owens, Wendt, Rabel and Kaelble (OWRK) method:

$$\gamma_{sl} = \gamma_s + \gamma_l - 2\left(\sqrt{\gamma_s^D \cdot \gamma_l^D}\right) + \sqrt{\gamma_s^P \cdot \gamma_l^P} \tag{6.2}$$

This builds on the Young-Dupré equation (Eq. 3.2) in chapter 2. π_e is assumed to be negligible for the interfaces studied in these tests. This is justified by the fact that adsorption only occurs if surface free energy would be reduced as a result. This is the case for liquids characterized by surface energies similar or lower than that of the substrate. Such a situation results in very low contact angles (<10 °) [54]. Since all the contact angles measured int his series of testing were much larger, the effect of vapor deposition is discounted. The Young-Dupré equation thus reduces to:

$$\gamma_{sv} = \gamma_{sl} + \gamma_{lv}(\cos\theta) \tag{6.3}$$

We are therefore left with one unknown variable to determine (γ_{SL}) in order to calculate the surface free energy of the metal which is where the OWRK method becomes useful. With at least two liquids with known disperse and polar parts of the surface tension, it is possible to calculate γ_{SL}.

The surface energy values calculated using this method are shown below in figures 6.11a and in 6.11b. It is evident in general that pretreating a hot-dip galvanized surface or MagiZinc® surface, be it with H_2TiF_6 or with H_2ZrF_6, results in an increase in the overall surface energy compared to the untreated sample. The practical implication of this is that treating any of the two galvanized steel substrates form Tata Steel with either Ti or Zr conversion treatments increases their surface free energy which in turn increases coating adhesion.

The dispersive contribution to the surface energy is shown in blue while the dispersive contribution is shown in orange. Here, we reiterate that the polar component of surface energy is representative of Coulomb interactions between surface species while the dispersive component represents fluctuating temporary interactions such as van der Waals interactions.

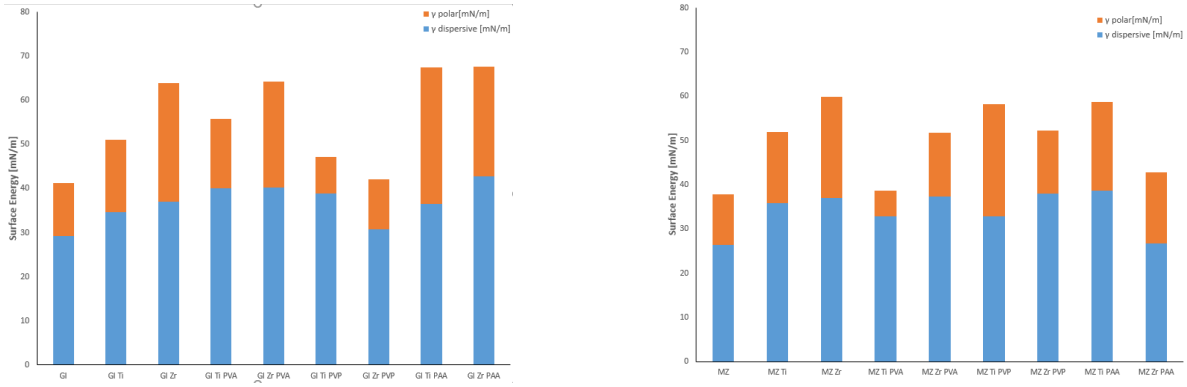

(a) GI **(b)** MagiZinc®

Figure 6.11: Surface energy for each sample derived from contact angle measurements according to Equation 6.3

To test this thesis, the relation between surface energy results and the pull-off adhesion test results was investigated. This comparison was performed rudimentarily by plotting the pull-off adhesion failure strength as a function of the calculated work of adhesion for each sample. Work of adhesion was calculated as follows:

$$W_a = 2\sqrt{\gamma_1^D \gamma_2^D} + 2\sqrt{\gamma_1^P \gamma_2^P} \tag{6.4}$$

Both graphs evince a general positive correlation between the parameters. Fitting of the data was not performed as more concrete knowledge of the specific factors contributing to the observed adhesion strengths is required.

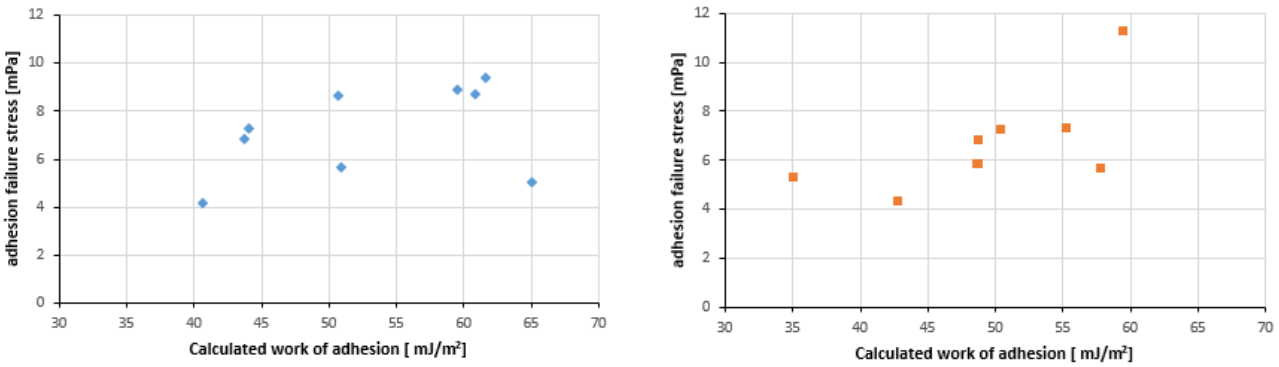

Figure 6.12: Surface energy values calculated for **(a)** conventional GI and **(b)** MagiZinc®

These results confirm that the changes that the different polymer additives render to the surface chemistry have a significant effect on adhesion. The surface free energy has also been proven to be a more reliable predictor of coating adhesion than surface roughness is.

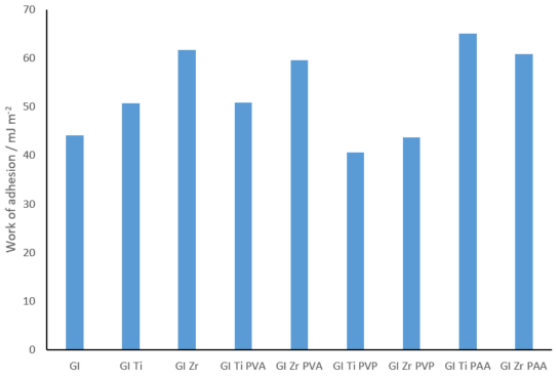

(a) MagiZinc®

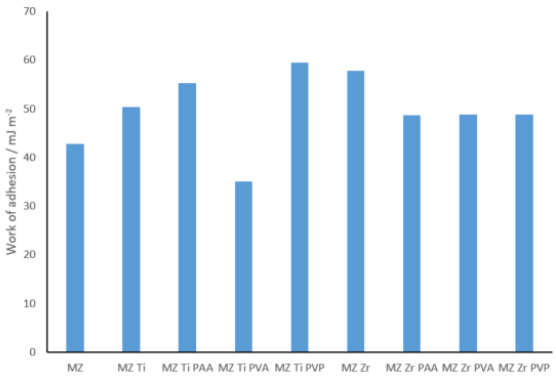

(b) GI

The results from the AFM, ATR/FTIR and XPS tests correspond each other suggesting that chemical interactions play a more dominant role in determining the adhesion strength achieved in a specific coating system than does the surface roughness. Therefore in the consideration of optimizing coating adhesion to galvanized steels, the primary concern should be the tuning the type as well as relative composition of the chemical species present at the interface with the coating.

6.2 Corrosion inhibition by green corrosion inhibitors

6.2.1 Potentiodynamic polarization

Figure 6.14 below shows the polarization curves of MagiZinc in the various inhibitor solutions. All significant changes for all inhibitors occur only in the cathodic branch. This indicates that the mechanism by which inhibition is achieved for each of the inhibitors tested is via inhibition of the cathodic reaction. No significant changes to the corrosion potential was observed.

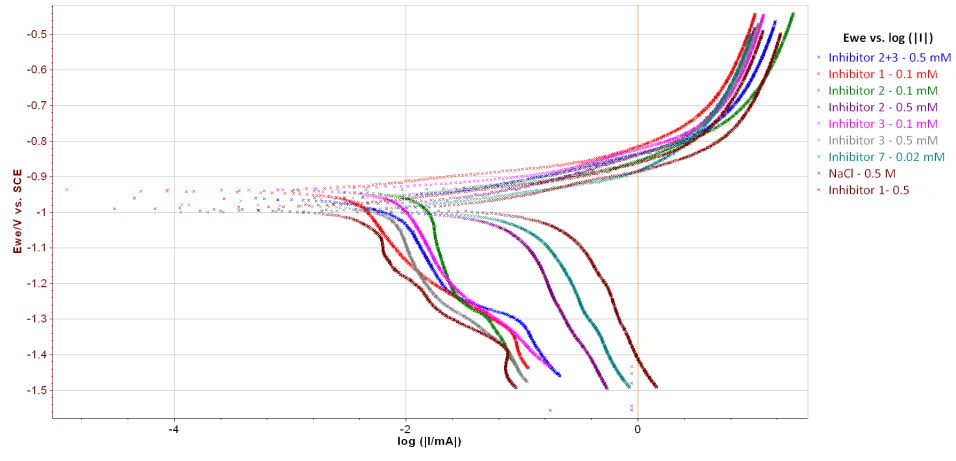

Figure 6.14: Polarization curves of MagiZinc with and without inhibitors

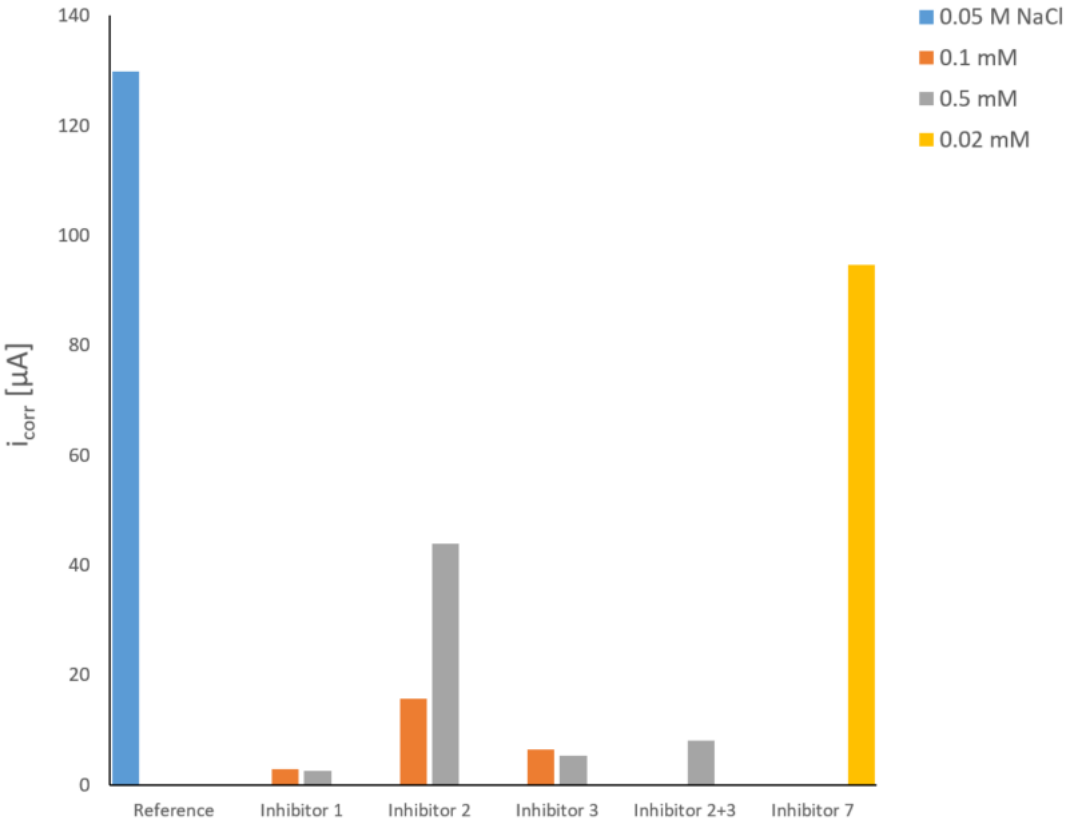

Figure 6.15: corrosion current density of MagiZinc in various inhibitor solutions

Tafel extrapolation was performed on each of these curves to determine corrosion current density, i_{corr}. These values are shown below in Figure 6.15. From these values the inhibitor efficiency of each inhibitor was calculated. The calculation is as follows:

$$\text{Inhibitor efficiency } (\%) = \frac{100 \cdot (i_{corr,uninhibited} - i_{corr,inhibited})}{i_{corr,uninhibited}} \tag{6.5}$$

The corrosion inhibitor efficiency calculated for each inhibitor is shown below in Figure 6.16:

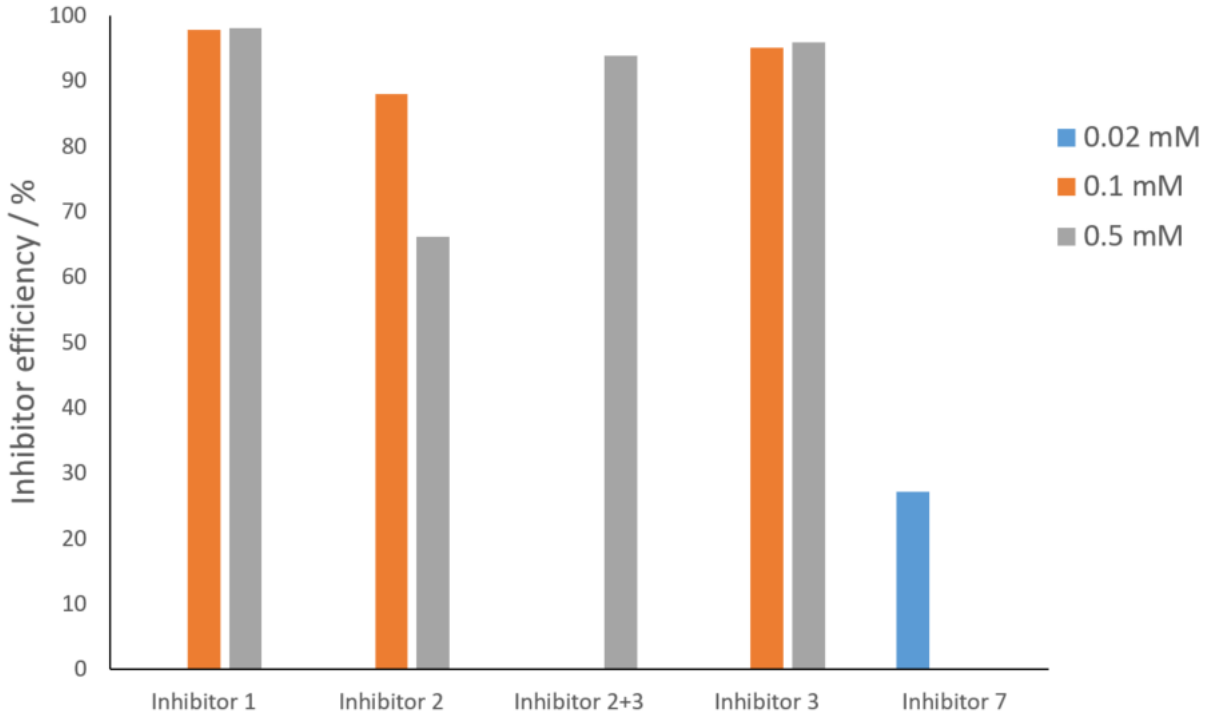

Figure 6.16: Calculated corrosion inhibition efficiency of each inhibitor

The highest corrosion inhibition efficiency was achieved with Inhibitor 1, an inhibitor comprising mainly silicate and calcium oxide. At 0.1 M, inhibition efficiency at 97.77% and did not increase significantly when the inhibitor concentration was increased to 0.5M. Inhibitor efficiency increased by 0.25% to 98.02%.

Similar inhibitor efficiency was observed for Inhibitor 3 which was also a silicate and calcium oxide pigment. This inhibitor had an efficiency of 95.09% at 0.1 M which increased to 95.97%. Inhibitor 2, composed of polyphosphates and silicates proved to be of interest due to the fact that its efficiency reduced when concentration was increased. This points toward the possibility of an optimum concentration beyond which the inhibition capability of the pigment diminishes possibly due to some competing mechanism. Inhibitor 7, based on zinc oxide and polyphosphate had the lowest inhibitor efficiency. This could however be attributable to the low concentration that was used compared to the other inhibitors.

6.2.2 Linear polarization resistance (LPR)

Figure 6.17 below shows the polarization resistance (R_p) measured for each sample over a week. Except for Inhibitor 2 at 0.5 mM concentration, all the inhibitors at each tested concentration increase the polarization resistance. The lower concentration for Inhibitor 2 is not included because the measurements obtained were unstable - possibly due to the amount added being too low for stable behaviour. For the same reasons, the measurements for Inhibitor 1 at both concentrations tested (0.1 and 0.5 mM) are not displayed in Figure 6.17.

Inhibitor 3 at a concentration of 0.5 mM exhibits a gradual increase of R_p values after about 40 hours which continues until the end of the measurement after 150 hours. This is interpreted as effective

inhibition of corrosion by the passive film commencing after 40 hours. Increasing the concentration Inhibitor 3 to 0.5 mM speeds up passive film formation. The R_p value starts to increase and appears to be rising still after 150 hours. This may be interpreted as the commencement of corrosion inhibition by passive film formation after about 20 hours. Film growth continues even up to 150 hours, leading to R_p values which eventually exceeding the performance of Inhibitor 2 0.5 mM after 100 hours (where the two plots intersect) and reaching a value of 2500 Ω cm^{-2} after 150 hours. This agrees with the results from the LPR tests which shows Inhibitor 3 at both concentrations having the highest efficiency. With the combination of inhibitors 2 and 3, (0.5 mM), R_p values recorded eventually reach a stable value of approximately 2000 Ω cm^{-2} after approx. 100 hours.

Inhibitor 7 also increases the R_p values relative to the reference. However, it is the only inhibitor tested for which, over the entire period of measurement, the polarization resistance is constantly decreasing. This behaviour is line with the inhibitor efficiency calculated for Inhibitor 7 from the potentiodynamic polarization measurement which is the lowest of all the inhibitors.

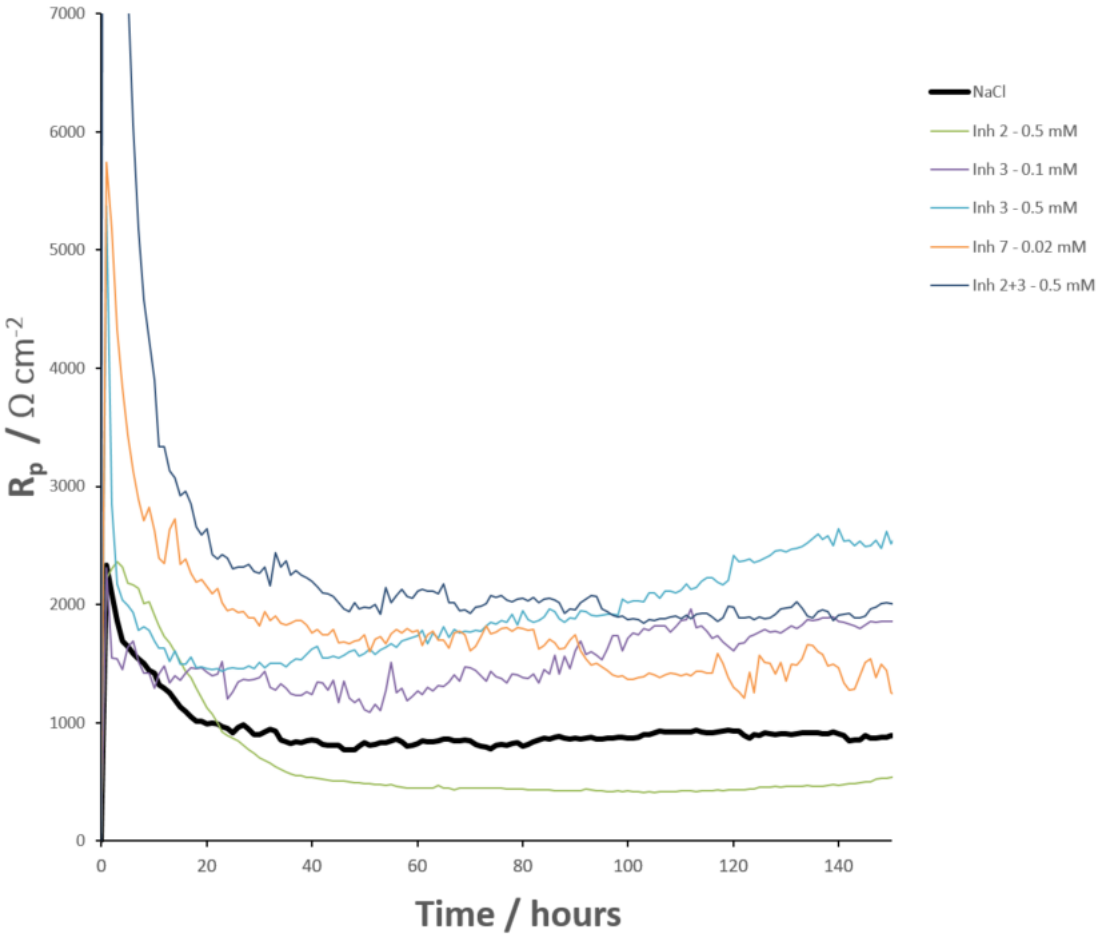

Figure 6.17: Polarization resistance curves for inhibited samples

In general, for the valid tests, the performance of the inhibitors in linear polarization testing agrees with those obtained from potentiodynamic polarization.

6.2.3 Electrochemical impedance

The polarization resistance values from EIS measurements are shown below in Figure 6.18. Inhibitor 1 is left out of the graph because as with the LPR measurements, the system was unstable over the course of measurement probably owing to insufficient amount of inhibitor added to the electrolyte. The results show that after about 50 hours, the protection of the combination of inhibitors 2 and 3 at a concentration of 0.5 mM is the most effective. Initially, Inhibitor 3 has the highest R_p values. These decrease gradually over time to below those for Inhibitor 2+3, reaching a stable value around 9000 Ω cm^{-2}, much higher than was observed in the LPR measurements.

An interesting observation is made for the solution containing Inhibitor 3 at a concentration of 0.1 mM. Almost no additional polarization resistance is observed until after 150 hours at which a sudden increase in the R_p value is observed. The value increases to approx. 3300 Ω cm^{-2}. Besides this inhibitor, all other inhibitors appear to provide significant corrosion inhibition on the MagiZinc substrate.

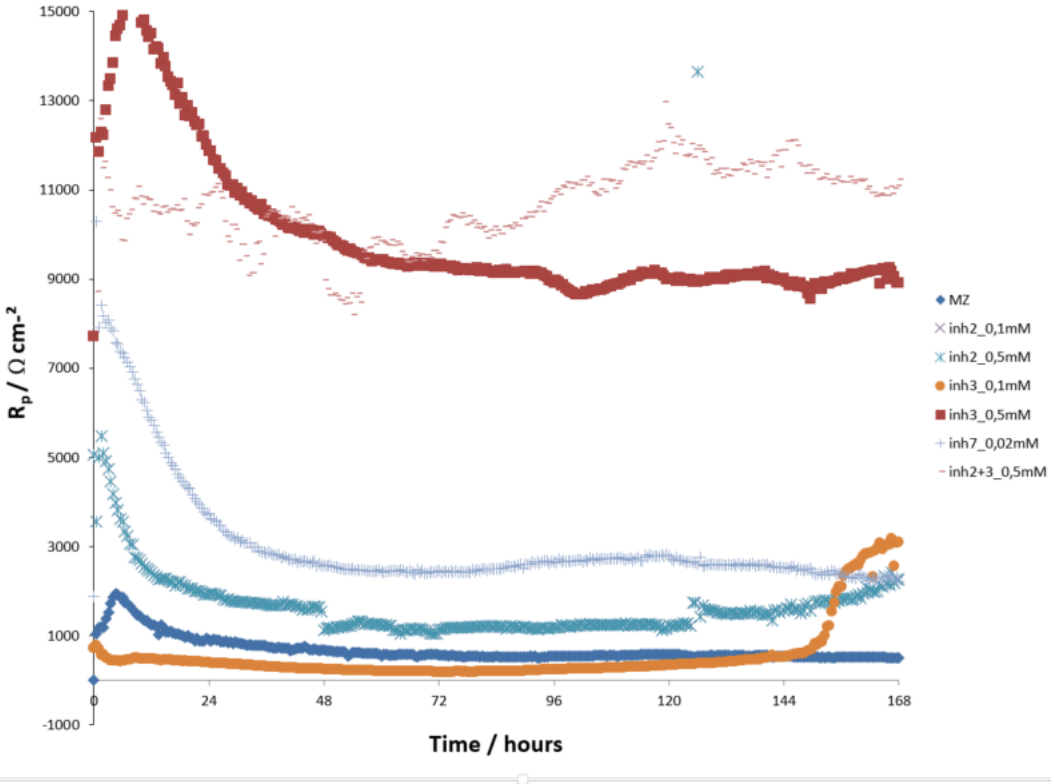

Figure 6.18: Polarization resistance as determined for electrochemical impedance spectroscopy for MagiZinc®

Chapter 7

Conclusions

The work performed over the course of this project has lead to several findings regarding the use of polymer additives in conversion treatments and also, regarding the suitability of a certain class of green inhibitors for MagiZinc and HDG galvanized steel. The results gathered in this work point toward promising performance in terms of polymer additives as adhesion enhancers as well as of green corrosion inhibitors. These, therefore, warrant further study.

At the end of this study the following questions have been addressed:

1. *How do titanium and zirconium compare as conversion coatings with regard to improving adhesion of organic coatings to the metal surface?*

   It is apparent that the relative performance of each pretreatment is highly dependent on the specific composition of the substrate in question. In this project, organic coatings on MagiZinc exhibit considerably stronger adhesion on substrates treated with H_2TiF_6 in comparison to samples treated with H_2ZrF_6. This is generally also true even with the incorporation of polymer additives for two out of the three additives tested (PAA and PVP).

   On conventionally galvanized steel, however, substrates treated with H_2ZrF_6 exhibit significantly better adhesion performance compared to H_2TiF_6. A possible reason for this is that on MagiZinc, Ti-treatment preferentially dissolves A- and Mg-rich phases, thereby enriching the surface zinc composition which proves to be beneficial for adhesion strength.

2. *How is adhesion on a galvanized steel surface influenced by incorporating organic additives in the conversion layer?*

   Some polymer additives do improve organic coating adhesion provided they are appropriately matched with the substrate and conversion coating chemistry. Evidence of this is seen in the varied results obtained for GI versus on MZ. The effect of organic additives is beneficial to coating adhesion on MagiZinc. Whereas on GI, they reduce the strength of coating adhesion.

- In general, roughness plays no significant role in the determination of coating adhesion strength. XPS, FTIR and AFM tests provide strong evidence that the strength of organic coatings to conversion-treated layers is largely dependent on the chemical interactions at the interface.
- It is also apparent that the quantity of cations that are deposited from the conversion solution are a decisive factor of adhesion strength. A higher proportion of conversion cations on the surface corresponds to stronger coating adhesion.

3. *In what way, if at all, is corrosion behaviour affected by the corrosion inhibitors studied?*
   Silicates, calcium ion exchange pigments, zinc oxide and phosphates all function as cathodic inhibitors. They slow down the rate of the cathodic reaction and in this way, reduce the corrosion current density.

4. *Which green corrosion inhibitors of those studied are most suitable for corrosion protection protection on MagiZinc?*
   For MagiZinc, calcium ion-exchanged silicates are the most suitable of the pigments studied in this project as corrosion inhibitors.

7.1 Recommendations

In practice, during actual application, tensile testing of adhesives is not as straightforward as it appears at first glance. It is nearly impossible achieve uniform stress distributions in such testing. This is only achievable if both the coating and the substrate have the same elastic modulus. A more suitable test would be the peel test. While pull-off testing is beneficial as a quantification method for adhesion testing, it should be used as a complementary test method.

Acid cleaning has been found to provide comparable and even better results for removing the contamination layer from substrates compared to alkaline cleaning. It would be of interest in future studies to examine and compare the two types of cleaning to determine the effect on cleaning efficiency, the subsequent conversion coating and adhesion of organic coatings.

Based on the indications towards the dominance of chemical interactions as a determinant of the strength of organic coating adhesion rather than surface roughness, further study is required. It would be worthwhile to investigate the specific chemistry of polymer additives studied and the exact nature of their chemical interactions with the organic coating. Gaining a detailed understanding of these interactions would facilitate a more precise determination of the appropriate additives for a specific substrate and coating system.

FTIR analysis of converted surfaces to determine species formed on surface after pretreatment. This would be beneficial towards understanding the exact changes rendered to the surfaces by the polymer additives.

One limitation of the pull off test is with the use of adhesives. There is a likelihood that the coating compound may react with the adhesive depend on their chemistry. This could significantly alter the bond strength especially given the low thickness of the coating investigated. It was assumed in this project that such effects were negligible if present at all.

Bibliography

[1] I. Milozev and G. S. Frankel. Review - conversion coatings based on zirconium and/or titanium. *Journal of the Electrochemical Society*, 165(3):C127–C144, 2018.

[2] Terrence R. Giles and Donald Vonk. The next generation of conversion coatings. *Encontro e Exposição Brasileira de tratamento de superficie*, 2012.

[3] Perluigi Molajoni and Adam Szewczyk. Indirect trade in steel: definitions, methodology and applications, Apr 2012.

[4] World Steel Association. *World Steel in Figures 2018*. 2018.

[5] Gerhardus Koch, Jeff Varney, Neil Thompson, Oliver Moghissi, Melissa Gould, and Joe Payer. International measures of prevention, application and economics of corrosion technologies study, 2016.

[6] J. Cerezo, I. Vandendael, R. Posner, K. Lill, J. H. W. de Wit, J. M. C. Mol, and H. Terryn. Initiation adn growth of modified zr-based conversion coatings on multi-metal surfaces. *Progress in Organic Coatings*, pages 284–289, 2013.

[7] L. Sziràki, E Szóc, Zs. Pilbáth, K. Papp, and E. Kálmán. Study of the initial stage of white rust formation on zinc single crystal by eis, stm/afm and sem/eds techniques. *Electrochimica Acta*, 46:3743–3754, 2001.

[8] Michel Keddam. Anodic dissolution. In Philippe Marcus, editor, *Corrosion Mechanisms in Theory and Practice*, pages 149–216. CRC Press, 3 edition, 2012.

[9] Arlene Courtney. Pourbaix diagrams, 2008.

[10] R. Winston Revie and Herbert H. Uhlig. *Corrosion and Corrosion Control: An Introduction to Corrosion Science and Engineering*. John Wiley and Sons, 4 edition, 2008.

[11] A. Vimalanandan, A. Bashir, and M. Rohwerder. Zn-mg and zn-mg-al alloys for improved corrosion protection of steels: Some new aspects. *Materials and Corrosion*, 64, 2014.

[12] Romina Krieg, Michael ROhwerder, Stefan Evers, Bernd Schuhmacher, and Janine Schauer-Pass. Cathodic self-healing at cut edges: The effect of zn2 $^{+}$ and mg2 $^{+}$ ions. *Corrosion Science*, 65, 2012.

[13] Peng Bicao, Wang Jianhua, Su Xuping, Li Zhi, and Yin Fucheng. Effects of zinc bath temperature on the coatings of hot-dip galvanizing. *Surface and Coatings Technology*, 202:1785–1788, 2008.

[14] The GalvInfo Center. Galvinfonote 2.4.1: Zinc bath management on continuous hot-dip galvanizing lines. *GalvInfoNotes*, 2017.

[15] Kenji Katoh, Hidetoshi Shindo, Takashi Yashiki, Kazumi Nishimura, and Hiroyasu Ishimito. Development of zn-mg-alloy-coated anti-corrosion steel plate for oil storage. In *Nippon Steel Technical Report No. 87*. Nippon Steel and Sumitomo metal, 2003.

[16] M.E. Kuperus. *The delamination behaviour of dross build-up structure on submerged hardware in Zn-Al and Zn-Mg-Al baths*. PhD thesis, Delft University of Technology, 2018.

[17] D. Gervasio, I. Song, and J. H. Payer. Determination of the oxygen reduction products on astm a516 steel during cathodic protection. *Journal of Applied Electrochemistry*, 28:979–992, 1997.

[18] Henry Leidheiser, Wendy Wang, and Lars Igetoft. The mechanism for the cathodic delamination of organic coatings from a metal surface. *Progress in Organic Coatings*, 11:19–40, 1983.

[19] R.A. Dickie. Chemical studies of the organic coating-steel interface after exposure to aggressive environments. In Ray A. Dickie and F. Louis Floyd, editors, *Polymeric Materials for Corrosion Control*, pages 136–154. American Chemical Society, 1985.

[20] J. S. Hammond, J..> Holubka, J. E. deVries, and R. A. Dickie. The application of x-ray photo-electron spectroscopy to a stuy of interfacial composition in corrosion-induced paint de-adhesion. *Corrosion Science*, pages 239–253, 1981.

[21] N. W. Khun and G. S. Frankel. Effects of surface roughness, texture and polymer degradation on cathodic delamination of epoxy coated steel samples. *Corrosion Science*, 67:152–160, 2013.

[22] Mirghasem Hosseini, Habib Ashassi-Sorkhabi, and Heshmat Allah Yaghobkhani Ghiasvand. Corrosion protection of electro-galvanized steel by green conversion coatings. *Journal of Rare Earths*, 25(5):537–543, 2007.

[23] United States Department of Labor OSHA. Hexavalent chromium, 2013.

[24] V. S. Sastri. *Green Corrosion Inhibitors: Theory and Practice*. Wiley, 2011.

[25] J. A. Petit, G. Chatainer, and F. Dabosi. Inhibitors for the corrosion of reactive metals: Titanium and zirconium and their alloys in acid media. *Corrosion Science*, 21:279–299, 1981.

[26] L. I. Fockaert, P. Taheri, S. T. Abrahami, B. Boelen, H. Terryn, and J .M. C. Mol. An in situ study of zirconium-based conversion treatment on zinc surfaces. *Applied Surface Science*, 423:817–828, 2017.

[27] G. W. Walter. A critical review of the protection of metals by paints. *Corrosion Science*, 26, 1986.

[28] C. H. Hare. Corrosion control of steel by organic coatings. In R. Winston Revie, editor, *Uhlig's Corrosion Handbook*, chapter 67, pages 971–983. John Wiley & Sons, 2011.

[29] R. A. Dickie. Paint adhesion, corrosion protection, and interfacial chemistry. *Progress in Organic Coatings*, pages 3–22, 1994.

[30] W. Funke. *JOCCA*, 68, 1985.

[31] Alphonsus V. Pocius. *Adhesion and Adhesives Technology*. Hanser Publishers, 2012.

[32] Maurice Brogly. Forces involved in adhesion. In L.F.M. da Silva, A. Öchsner, and R.D. Adams, editors, *Handbook of Adhesion Technology*. Springer, 2018.

[33] Lothar S. Sander, Edward M. Musingo, and William J. Neill. Composition and method for non-chromate coating of aluminum, 1988. US4921552A.

[34] Philip D. Deck, Molly Moon, and Richard J. Sujdak. Investigation of fluoacid based conversion coatings on aluminium. *Progress in Organic Coatings*, 34:39–48, 1998.

[35] Winfried Wichelhaus, Bernd Schenzie, and Heike Quellhorst. Method for providing metal surfaces with protection against corrosion, 2003. US20030150524A1.

[36] David Y. Dollman, Shawn E. Dolan, and Lester E. Steinbrecher. Composition and process for treating metal, 1992. US5534082A.

[37] Tanaka Tadashi and Ayusawa Saburo. Antirusting surface treating method for iron and steel products, 1960. US3132055A.

[38] Daisuke Fujimoto Satoshi Miyamoto, Toshiko Nakazawa. Zinc phosphate-containing surface conditioning agent phosphate conversion-treated steel plate and painted steel plate, and zinc phosphate dispersion, 2004. US20040011429A1.

[39] Zaki Ahmad. Corrosion control by inhibtion. In *Principles of Corrosion Control and Corrosion Engineering*, chapter 6, pages 352–381. Butterworth-Heineamann, 2006.

[40] R.N. Parkins. Corrosion inhibition. In J. Bockris, Brian E. Conway, Ernest Yeager, and Ralph E. White, editors, *Electrochemical Materials Science*. Springer, 1981.

[41] David E. J. Talbot and James D. R. Talbot. *Corrosion Science and Technology*. CRC Press, 3 edition, 2018.

[42] Camila G. Dariva and Alexandre F. Galio. Corrosion inhibitors - principles, mechanisms and applications. In Mahmood Aliofkhazraei, editor, *Developments in Corrosion Protection*. IntechOpen, 2014.

[43] Phillipe Marcus. *Corrosion Mechanisms in Theory and Practice*. CRC Press, 3 edition, 2011.

[44] O. Lahodny-Sarc and L. Kastelan. Inhibition of mild steel by polyphosphates. *Corrosion Science*, 16:25–34, 1976.

[45] R Naderi and M Attar. The inhibitive performance of polyphosphate-based anticorrosion pigments using electrochemical techniques. *Dyes and Pigments*, 80(3):349âĂŞ354, 2009.

[46] Rongchang Zeng, Zidong Lan, Linghong Kong, Yuanding Huang, and Hongzhi Cui. Characterization of calcium-modified zinc phosphate conversion coatings and their influences on corrosion resistance of az31 alloy. *Surface and Coatings Technology*, 205:3347–3355, 2011.

[47] I. M. Zin, S. B. Lyon, and V.I. Pokhmurskii. Corrosion control of galvanized steel using a phosphate/calcium ion inhibitor mixture. *Corrosion Science*, 45:777–788, 2003.

[48] F. Deflorian, L. Fedrissi, and P.L. Bonora. Corrosion protection performances of coil coatingproducts with ion-exchange pigments. In *Proceedings ofthe Symposium on advances in Corrosion Protection by Organic Coatings III*, volume 97-41, pages 45–56. The Electrochemical Society, 1997.

[49] N. Granizo, M. I. Martin, F. A. Lopez, J. M. Vega, D. de la Fuente, and M. Morcillo. Chemical and structural changes of calcium ion exchange silica pigment in 0.5 mNaCl and 0.5 m Na_2SO_4 solutions. *Afinidad LXVIII*, 68, 2012.

[50] Thomas Lostak, Artjom Maljuschb, Bjorn Klink, Stefan Krebs, Matthias Kimpel, Jorg Flocka, Stephan Schulzc, and Wolfgang Schuhmann. Zr-based conversion layer on zn-al-mg alloy coated steel sheets: Insights into the formation mechanism. *Electrochimica Acta*, pages 65–74, 2014.

[51] Lee H. Pearson. Ir spectroscopy for bonding surface contamination characterization. In D. O. Thompson and D. E. Chimenti, editors, *Review of Progress in Quantitative Nondestructive Evaluation*, volume 9. Plenum Press, 1990.

[52] Sven Pletincx, Lena Trotochaud, Laura-Lynn Fockaert, Johannes M. C. Mol, Ashley R. Head, Osman Karslioglu, Hendrik Bluhm, Herman Terryn, and Tom Hauffman. In situ characterization of the initial effect of water on molecular interactions at the interface of organic/inorganic hybrid systems. *Sci. Rep.*, 7:45123, 2017.

[53] R. R. L. De Oliveira, D. A. C. Albuquerque, T. G. S. Cruz, F. M. Yamaji, and F. L. Leite. *Measurement of the Nanoscale Roughness by Atomic Force Microscopy: Basic Principles and Applications*. Intech Open, 2012.

[54] Souheng Wu. *Polymer Interface and Adhesion*. CRC Press, 1982.

[55] P. Taheri, K. Lill, J. H. W. de Witt, J. M. C. Mol, and H. Terryn. Effects of zinc surface adicbase properties on formation mechanisms and interfacial bonding mechanisms of zirconium-based conversion layers. *Journal of Physical Chemistry*, 116(15):8426–8436, 2012.

[56] John Comyn. *Adhesion Science*. Royal Society of Chemistry, 1997.

[57] Authur G. Smith and Ray A. Dickie. Adhesion failure mechanisms of primers. *Ind. Eng. Chem. Prod. Res. Dev*, 17:42–44, 1978.

[58] François Baruthio. Toxic effects of chromium and its compounds. *Biological Trace Element Research*, 32:145–53, 1992.

[59] T. S. N. Sankara Narayanan. Surface pretreatment by phosphate conversion coatings - a review. *Review of Advanced Materials Science*, 2005.

[60] Elcometer®. *User Guide: Elcometer 456 Coating Thickness Gauge*, 2018.

[61] SAE International, editor. *MagiZinc - The New High Performance Coating for Steel in the BIW and Closures*. SAE international, 2016.

[62] Hans-Henning Strehblow. Fundamentals of corrosion. In *Corrosion Mechanisms in Theory and Practice*. CRC Press, 2011.

Appendix A

Impedance spectroscopy results

In this appendix, the results from the electrochemical impedance spectroscopy tests are presented.

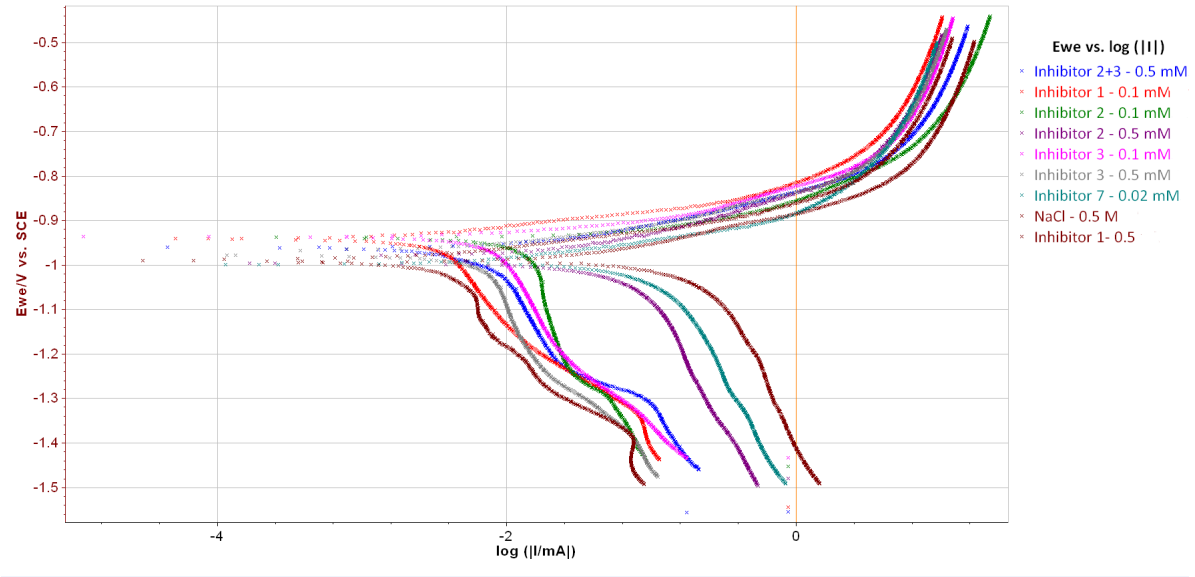

Figure A.1: Polarization curves for MagiZinc in 0.05 M NaCl solutions containing various inorganic green inhibitor solutions

Appendix B

Relevant data from literature

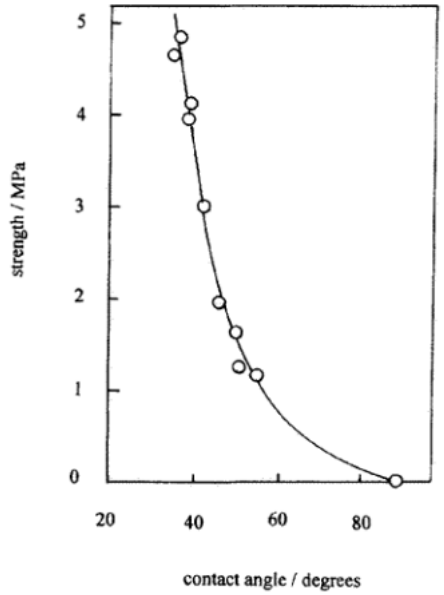

Figure B.1: Variation of adhesion strength with contact angle at polyethylene lap joints with epoxy adhesive from [56].

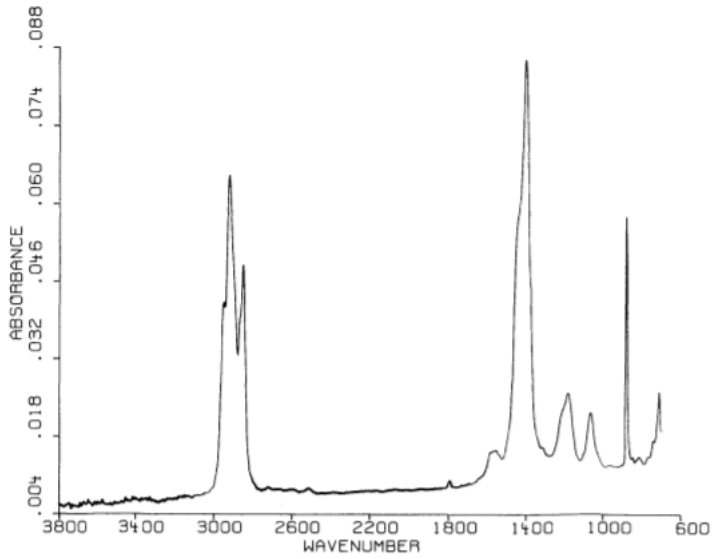

Figure B.2: IR spectrum of a typical grease contaminant adapted from [51]